ALLEN INSTITUTE for BRAIN SCIENCE
Fueling Discovery

Allen Mouse Common Coordinate Framework

TECHNICAL WHITE PAPER:
ALLEN MOUSE COMMON COORDINATE FRAMEWORK AND REFERENCE ATLAS

OVERVIEW

The Allen Mouse Common Coordinate Framework (CCF) is an essential tool to display the structure of the mouse brain. It has been used for large-scale data mapping, quantification, presentation, and analysis and has evolved in complexity and resolution through the creation of multiple versions. The first version (in 2005) of the CCF (CCF v1) was created to support the product goals of the Allen Mouse Brain Atlas (**Figure 1**) (Lein *et al*., 2007). The framework was based upon the Allen Reference Atlas (ARA) specimen (Dong, 2008) in which a 3-D volume was reconstructed using 528 Nissl sections of a near complete brain. Approximately 200 anatomical structures were extracted from the 2-D atlas drawings to create 3-D references for annotations. A second version (in 2011) of a refined CCF (CCF v2) was constructed to support the volumetric spatial mapping requirements of the Allen Mouse Brain Connectivity Atlas (Oh *et al*., 2014) where a double-sided and more deeply annotated framework was needed (**Figure 1**). During the development, flaws in the 3-D reconstructions were corrected and a hemi-brain volume was mirrored across the mid-line to create a symmetric space. Eight hundred and sixty anatomical structures were extracted and interpolated to create symmetric 3-D annotations. These corrections greatly improved the accuracy of annotation as compared with coronal 2-D images; however, when viewed in sagittal and horizontal planes, the boundary areas were still not smooth, as an artifact of 2-D to 3-D illustration file conversion.

In 2012, the Allen Institute launched a comprehensive plan to investigate brain function. This included cataloguing cell types and understanding the relationships between those different kinds of cells. A next generation CCF, 3-D digital mouse brain atlas was created to support and integrate multimodal data generated as part of this plan. CCF Version 3 (v3) is based on a 3-D 10μm isotropic, highly detailed population average of 1,675 specimens. This average template contains 1,319 coronal, 619 sagittal and 799 horizontal plates. By overlaying multiple reference data sets with the average template, CCF v3 was manually reconstructed using the 3-D drawing software ITK-SNAP. The final CCF product consists of 662 annotated structure volumes, including gray matter, white matter and ventricles. Overall, 242 cortical and 330 subcortical gray matter, 82 fiber tracts, and 8 ventricle and associated structure volumes were delineated natively in 3-D. CCF v3 completely replaces CCF v2 and is freely accessible, providing an anatomical infrastructure for the quantification, integration, visualization and modeling of the large-scale data sets for the Allen Institute for Brain Science and the entire neuroscience community (CCF v3 portal).

This technical white paper describes the methods used to generate the CCF v3, including the creation of the anatomical template, reference data sets, new and updated structures, and 3-D annotation and processing.

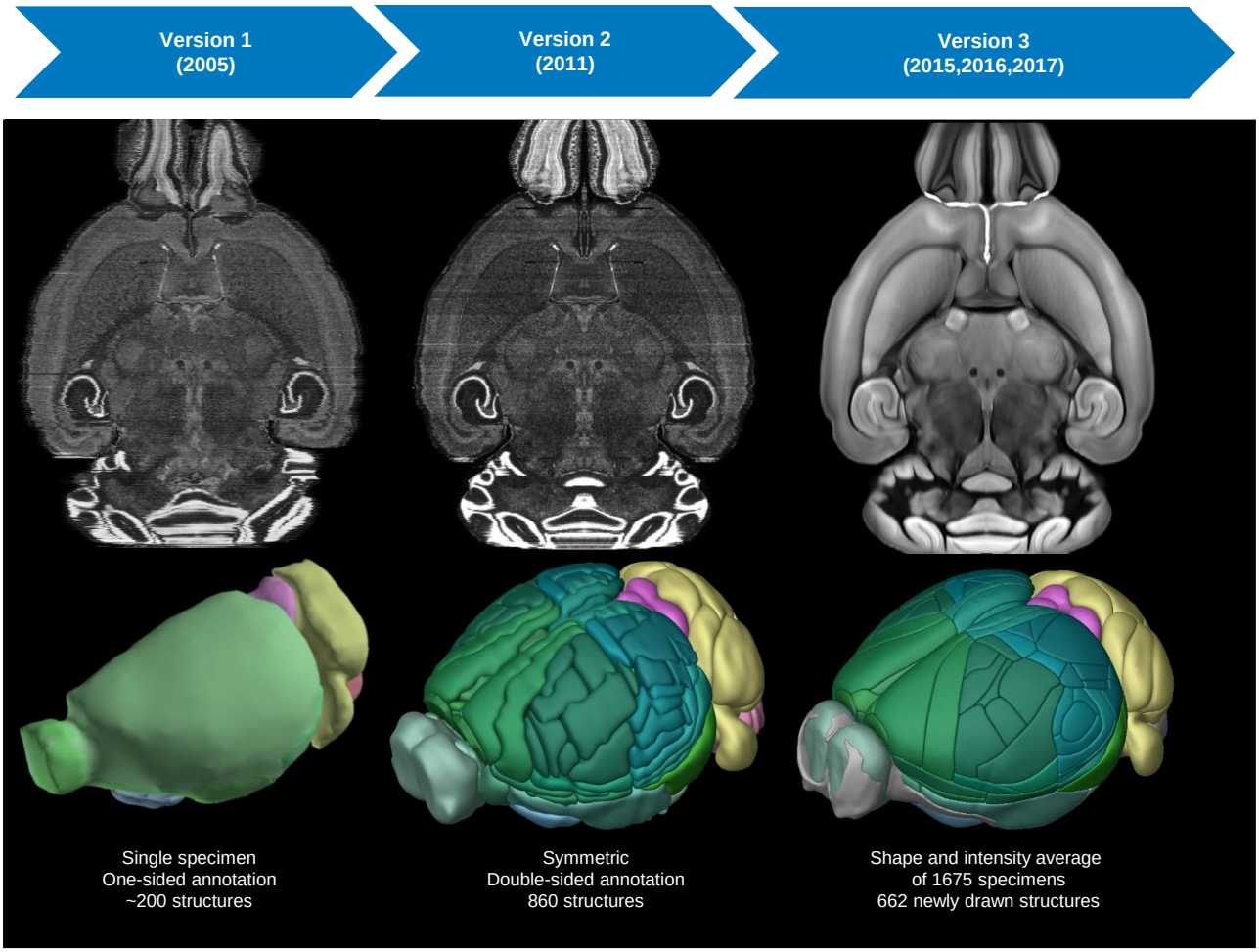

Figure 1. Evolution of the Allen Mouse Common Coordinate Framework.
The first version (2005) supported the Allen Mouse Brain Atlas and was based upon the Allen Reference Atlas specimen. A second version (2011) supported the Allen Mouse Brain Connectivity Atlas where a double-sided and more deeply annotated framework was needed. Version 3 (2017) of the Common Coordinate Framework is based on a population average of 1675 specimens and has 662 newly drawn 3-D structures.

CREATION OF THE ANATOMICAL TEMPLATE

The anatomical template of CCF v3 is a shape and background signal intensity average of 1675 specimens from the Allen Mouse Brain Connectivity Atlas (Oh *et al*., 2014). Specimens in the Allen Mouse Brain Connectivity Atlas were imaged using a customized serial two-photon (STP) tomography system, which couples high-speed two-photon microscopy with automated vibratome sectioning. STP tomography yields a series of inherently prealigned images amenable for precise 3-D spatial mapping.

A population average was created through an iterative process, averaging many brains over multiple cycles. This iterative process was bootstrapped by 12-parameter affine registration of specimens to the “registration template” created as part of the Allen Mouse Brain Connectivity Atlas data processing pipeline (Kuan *et al*. 2015). The “registration template” effectively provides initial orientation and size information to this process. To create a symmetric average, each of the 1675 specimens was flipped across the mid-sagittal plane and the flipped specimens were used as additional input to the averaging process. The total 3350 (= 2 x 1675) hemispheres were registered and averaged to create the first iteration of the CCF v3 anatomical template.

Following the method in (Fonov 2011), two steps were performed during each iteration: (1) each specimen was deformably registered to the template and averaged together; (2) the average deformation field over all specimens was computed, inverted, and used to deform the average image created in (1). This shaped normalized average was then used as the anatomical template in the next iteration. This algorithm continues until the mean magnitude of the average deformation field was below a certain threshold. For computational efficiency, the method was first applied to the data down sampled to 50µm resolution until convergence was reached. This result was then used as input to the 25µm processing round. In the final step, the specimens were resampled at 10µm resolution and averaged to create the final 3-D volume.

The anatomical template possesses two properties: (a) the intensity difference between the average and each transformed specimen was minimized and (b) the magnitude of all the deformation fields used to transform each specimen was minimized. The anatomical template is thus the average shape and average appearance of the population of 1675 specimens and shows remarkably clear anatomic features and boundaries for many brain structures.

REFERENCE DATA SETS

Reference data sets are crucial for confirming the identification of anatomical structures visible in the anatomical template and also for drawing those that are not visible in the anatomical template. The following were used to delineate gray matter and white matter structures in 3-D.

1. **Allen Mouse Brain Connectivity Atlas - Projection Data** (connectivity.brain-map.org): This data set shows the projections and projection topographies from given anatomical structures. Methods for data generation have been previously described in detail (Oh *et al*., 2014) and can be found in the Technical White Papers located in the Documentation tab. STP tomography imaging enables accurate registration of the data to the average template for delineation of anatomical structures for CCF v3.

2. **Allen Mouse Brain Connectivity Atlas - Reference Data** (connectivity.brain-map.org): Reference data includes two histology datasets (Nissl- and AChE-stained sections) and three immunohistochemistry datasets (SMI-32 and Parvalbumin, NeuN and NF-160, calbindin 1 and SMI-99 double-stained specimens). See the Reference Dataset white paper located in the Documentation tab for more details. Reference data were registered to the average template using customized methods. Registration accuracy was limited due to the modest amount of deformation and tissue damage. Regardless, these datasets have great utility in providing anatomical details for delineating certain structures.

3. **Transgenic Mouse Data** (data not published): Transgenic cre driver mouse lines exhibiting differential tdTomato labeling in genetically-defined cell populations are important tools for anatomic delineation, particularly where structures and their borders cannot be distinguished using the anatomical template. For this version of the CCF, datasets using transgenic cre driver brains generated by the same perfusion and imaging procedures as in the Allen Mouse Connectivity Atlas were used, allowing easy integration of this data to the average template. Newly generated data from 58 transgenic lines were used to provide anatomical information for completing the targeted 3-D structural delineation for the final product.

4. ***In Situ* Hybridization (ISH) Data** (mouse.brain-map.org): Molecular markers have been a powerful tool for the delineation of brain structures (Lein *et al*., 2005; Lein *et al*., 2007; Dong, 2008). There are a number of genes that exhibit remarkably regionalized expression that were used to indicate borders in the anatomical template as well as confirm those previously delineated.

Updated and New Structures: The ARA anatomical ontology was used for the CCF v3 to maintain continuity for multiple products that are part of the Allen Brain Atlas Data Portal. Updates to the ARA ontology were made that included the addition of structures in the higher visual areas, specifically the anterior visual area (layers 1, 2/3, 4, 5, 6a, and 6b), laterointermediate area (layers 1, 2/3, 4, 5, 6a, and 6b), rostrolateral visual area (layers 1, 2/3, 4, 5, 6a, and 6b), and postrhinal area (layers 1, 2/3, 4, 5, 6a, and 6b) to the visual and posterior parietal area branches of the brain structure tree. In addition to the neocortex, 38 new subcortical gray matter structures,

not delineated in the ARA, were added. Except for the dorsal terminal nucleus (DT) and medial terminal nucleus (MT) of the accessory optic tract which exist in the ARA ontology, the nomenclatures of 36 structures were adopted from Paxinos and Franklin's mouse atlas (2001) and from recent literature (Ding, 2013; Martersteck et al., 2017; Quina et al., 2017). Five new fiber tracts were added to the ontology and annotated in 3-D space (see **Table 1**).

Structures drawn in 3-D were located throughout the brain, including in the isocortex (43 structures), olfactory areas (17 structures), hippocampal formation (25 structures), cortical subplate (10 structures), striatum (16 structures), pallidum (9 structures), thalamus (50 structures), hypothalamus (50 structures), midbrain (58 structures), pons (29 structures), medulla (46 structures), cerebellum (20 structures), fiber tracts (82 structures), and ventricular systems (8 structures). A detailed structure list is shown in **Table 1**.

3-D ANNOTATION AND PROCESSING

3-D Annotation

For the 3-D annotation, manual delineation of the anatomical template was a combined process of structure discovery and 3-D illustration carried out at various levels: consideration of individual structures, context of local structures and interface between adjacent structures (**Figure 2A**). Using anatomical template contrast features and fiducials from select supporting data (described below), structures were landmarked, illustrated serially, and cross-checked for accuracy. In certain cases, the process was modified to include previously-drawn structures (**Figure 2B**), which greatly increased anatomic accuracy and illustrative efficiency. Once completion of a structure group was achieved, all individual and local structure groups were merged (**Figure 2C**). At this stage, local aberrations such as boundary overlaps and structure gaps were considered at a brain-wide level and brought into alignment. The process was completed with a final evaluation of structures based on comparison with the component 2-D plates as well as the rendered 3-D composition.

ITK-SNAP (www.itksnap.org), a freeware 3-D annotation tool (Yushkevich *et al*., 2006), was utilized throughout the discovery and illustration processes. After loading the 10µm/voxel anatomical template, a region of interest (ROI) was identified provisionally in the given viewing planes (horizontal, sagittal, and coronal) by a neuroanatomist. Key anatomical features present in the template were observed, researched, and visually enhanced by the standardized employment of image adjustment tools provided in ITK-SNAP. When additional evidence was necessary, supporting data was registered and overlaid semi-transparently or launched in a parallel ITK-SNAP window for voxel-to-voxel tracking. Once an ROI is evaluated, the neuroanatomist produced a landmark segmentation (multi-planar 2-D delineations at regular intervals), which was given to illustrators who complete the segmentation serially and refine surface features to an appropriate level of maximum smoothness. The resulting structure was then compared back to the original landmark segmentation and either refined or submitted to the chief neuroanatomist for final approval. These were the principle mechanics for building CCF structures in ITK-SNAP. As additional structures were built, specialized macros for merging and splitting individual files were utilized to facilitate group delineations and form-fitting adjustments at local and global levels, respectively.

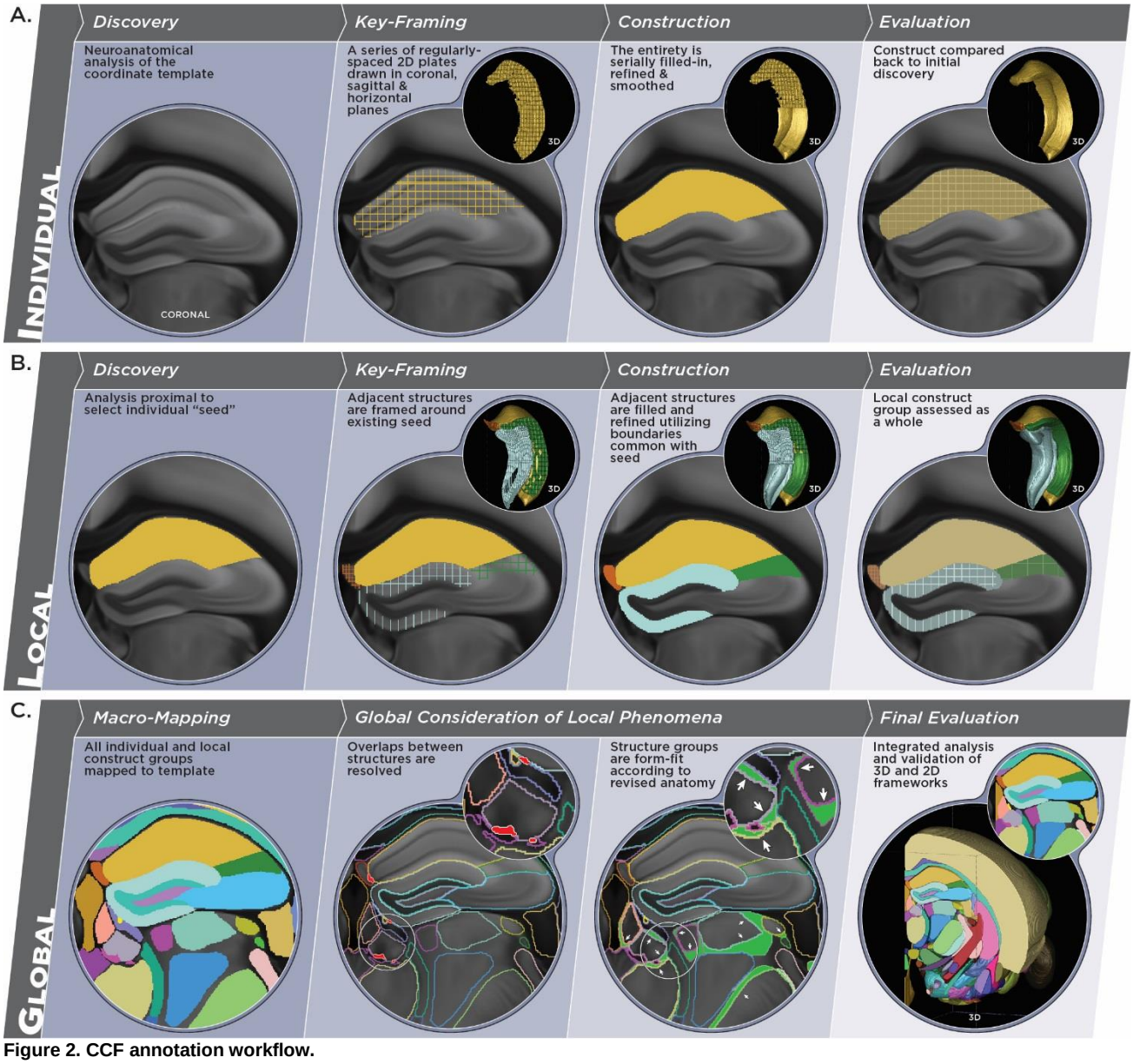

Figure 2. CCF annotation workflow.
A. Structures with sufficient individual context are identified (discovery), 3-dimensionally outlined (key-framing), filled-in (construction) and validated (evaluation). **B.** Where possible, building is then performed in direct context of individually-built structures, such as the hippocampus (shown). This aids the fill-in process and ensures seamless interlocking of the entire local structure group. **C.** After building at the individual and local levels, structures are finally brought together for negotiation in a single, brain-wide context. Once overlaps are resolved and structures appropriately form-fit, a final evaluation is performed to ensure overall accuracy in 2-D and 3-D frameworks.

Creating a Curved Cortical Coordinate System

As part of the construction of CCF v3, a curved cortical coordinate system was developed to enable the integration of information from different cortical depths. The construction started with a manual delineation of the isocortex. Definition of the isocortex used here was adapted from the ARA ontology (Dong, 2008). According to that definition, the isocortex is bordered rostroventrally by the main olfactory bulb (MOB), the accessory olfactory bulb (AOB) and the anterior olfactory nucleus (AON), laterally by the AON, the piriform area (PIR) and the entorhinal area (ENT), medially by the dorsal peduncular area (DP), the subiculum (SUB) and postsubiculum (POST), and caudally by the medial entorhinal (ENTm) area, and parasubiculum (PAR). Although the boundaries of isocortex were recognizable in the anatomical template itself, manual delineation was greatly facilitated by the addition of transgenic mouse brain data registered with the anatomical template. In this case,

calbindin expression (Calb1) was used (visualized by crossing the Calbindin1-2A-dgCre mouse line with the Ai14 reporter to label Calb1 positive cells with tdTomato fluorescent protein). Calb1 is strongly expressed throughout the isocortex, except in the ventral portion of the retrosplenial area (RSPv), and is weakly expressed in the paleocortex, including the entorhinal area (ENT) and the piriform area (PIR).

Figure 3 shows the anatomical template with overlaid reference data at select coronal levels, from rostral to caudal. Rostral isocortex (orbital area and agranular insular area) was separated from the olfactory bulb (MOB and AON) based on differential fluorescent signal (**Figure 3A**). Lateral isocortex (agranular insular area and perirhinal area) was separated from the AON, PIR, and ENT in a similar fashion (**Figure 3 A-D**). Compared to the lateral isocortex, medial isocortex has strong fluorescent signal only in the rostral part. Rostromedial isocortex (infralimbic area) was also separated from dorsal peduncular areas (DP) by fluorescent signal differences (**Figure 3B**). For the caudomedial portion of isocortex (RSPv), separation from SUB and POST was indicated by dramatic laminar differences observed in the anatomical template itself (**Figure 3D**). Fluorescence differences were again used in the caudal part of the isocortex (posterolateral visual area and RSPd) for separation with ENTm and PAR.

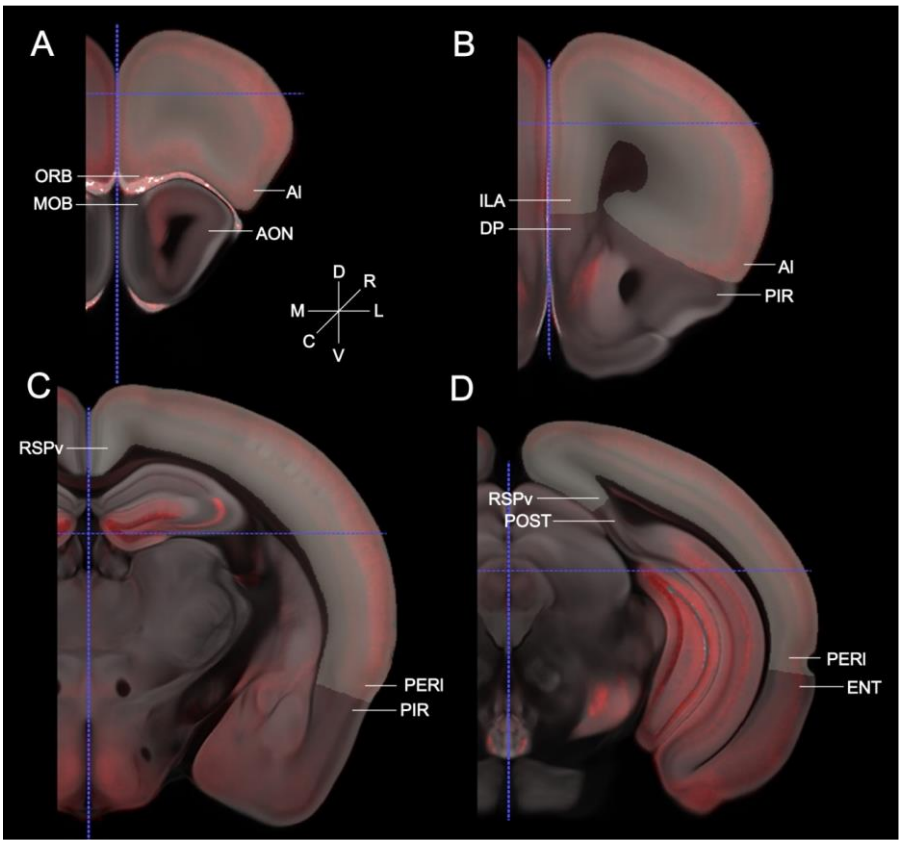

Figure 3. Delineation of the isocortex.
The transgenic reference data (Calbindin1-2A-dgCre) were overlaid with the anatomical template. Structures expressing tdTomato (a red fluorescent protein) were labeled in red. **A-D.** Examples show the boundaries of the isocortex at different levels from rostral to caudal. The border of the isocortex was indicated by sticks and the isocortex was painted in light yellow. Abbreviations: AI, agranular insular area; AON, anterior olfactory nucleus; C, caudal; D, dorsal; DP, peduncular area; ENT, entorhinal area; ILA, infralimbic area; L, lateral; M, medial; MOB, main olfactory bulb; ORB, orbital frontal area; PERI, perirhinal area; PIR, piriform area; POST, postsubiculum; R, rostral; RSPv, ventral part of the retrosplenial area; V, ventral.

After the borders of isocortex were defined, Laplace's equation was solved between pia and white matter surfaces resulting in intermediate equi-potential surfaces (**Figure 4A**). Streamlines were computed by finding orthogonal (steepest descent) path through the equi-potential field (**Figure 4B**). Information at different cortical depths can then be projected along the streamlines to allow integration or comparison. Streamlines were used to facilitate the annotation of the entire isocortex, including higher visual areas.

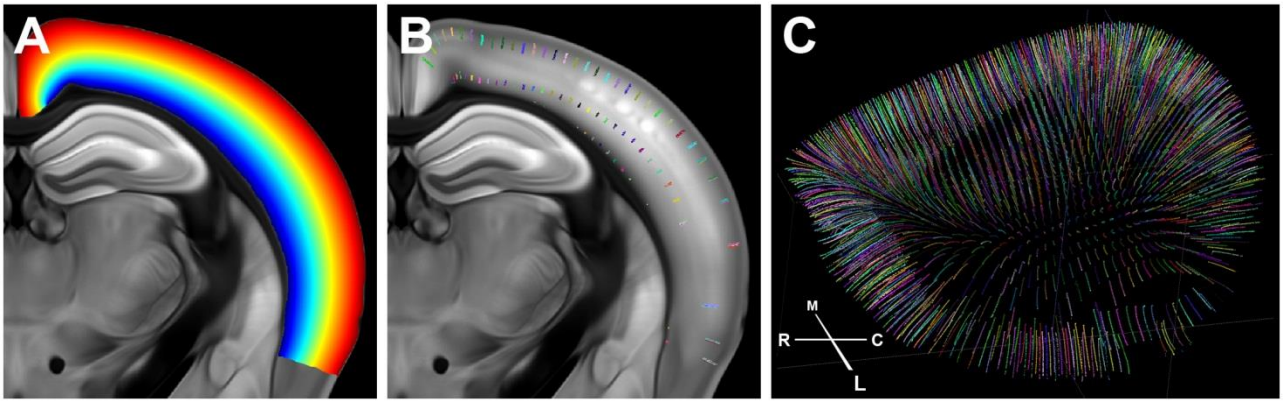

Figure 4. Curved cortical coordinate system.
A. Laplace's equation is solved between pia and white matter surfaces to generated intermediate equi-potential surfaces as analog to cortical depth. **B-C**. Streamlines are computed by finding a curved "orthogonal" path through the equi-potential field. Abbreviations: M, medial; L, lateral; R, rostral; C, caudal.

Annotation of the Isocortex in 3-D Space

The isocortex was annotated from surface views using the curved cortical coordinate system described above. The curved cortical coordinate system has an advantage in that it allows the translation of any point from 2-D surface views into 3-D space or vice versa. Thus, mapping isocortex from surface views is a different approach compared with conventional 3-D mouse brain atlases that are built from a series of 2-D coronal sections, such as the ARA (**Figure 1,** version 2). To guide annotation of cortical areas, three data sets were used: the average template, transgenic data and connectivity data. First, the higher visual areas were delineated by overlaying virtual callosal connections and the visuotopic map with the anatomical template. The transgenic and connectivity data were then used to delineate the rest of the isocortex. Finally, delineation of cortical layers was based on a combination of information in the anatomical template and selected transgenic markers. Using this supporting evidence, a total of 43 cortical areas and associated cortical layers were constructed in 3-D space (**Figure 1**, version 3).

Higher Visual Areas

In the ARA (Dong, 2008), the visual cortex consists of six anatomically defined visual areas drawn on a single, Nissl-stained specimen. Recent studies using tract-tracing and intrinsic signal imaging methods (Wang and Burkhalter, 2007; Marshel *et al*., 2011; Garrett *et al*., 2014) have shown that there are at least ten functional visual areas that contain complete visuotopic maps. These studies use flattened cortex surface views to exhibit distinguishable topographies of primary and higher visual areas. Since higher visual areas are impossible to distinguish in the anatomical template itself (**Figure 5A**), a similar surface mapping approach was taken to delineate higher visual areas in the CCF v3.

Since various angles provide different information regarding surface views, seven angles were chosen to cover the full extent of visual cortex and its closely related areas: top, bottom, rotated, medial, side, front and back. An example, top view, is shown in **Figure 5**. To generate surface views of the anatomical template, the highest intensity (brightest) voxel along a streamline was projected to its surface voxel counterpart. Additional reference data can be incorporated into the surface views by registering the data into the CCF and similarly projecting maximum intensity information to the surface using these streamlines.

Inspection of the anatomical template surface view revealed distinctly bright domains putatively representing the primary visual, somatosensory, auditory, and the retrosplenial areas (**Figure 5A**). Comparing data from expression-based transgenic mouse reporter lines (Nr5a1-Cre) and histological sections (SMI-32; a neurofilament antibody assay previously reported to stain these regions (Wang *et al*., 2011)), confirmed the presence and location of these areas, which were landmarked (**Figure 5B**). The darker regions between four landmarked areas contain higher visual areas.

To reveal higher visual areas, data from 26 stereotaxic injections located throughout retinotopic space in primary visual area were analyzed from the Allen Mouse Brain Connectivity Atlas. Images for each of the 26 injections were segmented and registered (Kuan *et al*., 2015) to obtain 3-D volumes of projection signal density. The 26 density volumes were combined to create a color-coded weighted source location map. For each injection, a "center" 3-D location was computed. At each voxel on the 3-D map, a weighted source location was computed as the weighted sum of injection center locations with the weights being the projection density value at the voxel arising from each of the different injections. Additionally, summed projection density over all injections was also computed for each voxel. The cortex was computationally normalized into a "sheet" with uniform depth. To create a surface view, signal within 10% to 50% of the uniform depth was considered. The maximum summed projection density voxel for each streamline was identified and the weighted source location of the maximum density voxel was projected to the surface of the sheet. To aid visualization, a weighted location was color-coded as follows: the HSV (hue-saturation-value) color wheel was mapped on to the primary visual area location such that magenta corresponds to the nasal visual field, cyan for temporal visual field and blue for lower visual field. Color at any intermediate location was interpolated from the HSV formula. A color-coded top view is shown in **Figure 5C**. This result recapitulates the previous finding in which higher visual areas were delineated based on their visuotopic maps (Wang and Burkhalter, 2007).

In addition to visuotopic maps, a virtual callosal projection pattern was generated using cortical stereotaxic injection data from the Allen Mouse Brain Connectivity Atlas. A virtual callosal map was created using 108 injections spanning the isocortex. A maximum projection density map was created by finding, at each voxel, the maximum density value over all injections. Since all injections in the Allen Mouse Brain Connectivity Atlas were in the right hemisphere, to create a callosal map, each dataset was flipped across mid-sagittal plane and treated as virtual left hemisphere injections. A surface view was then generated by considering only signal within 10% to 50% of the uniform cortical depth and projecting the largest maximum value to the surface of the cortical sheet. This projection pattern was employed for fixed landmark referencing, which is important because higher visual areas have unique spatial relationships with callosal projections from the opposite hemisphere. As shown in **Figure 5D**, callosal projections terminate at the borders between the primary visual area and the lateral and anterolateral visual areas, and at the border between the primary somatosensory area and the supplemental somatosensory area, while avoiding the rest of the primary visual area and barrel fields of the primary somatosensory area. A large acallosal zone is located on the lateral side of the primary visual area and a small acallosal ring is located rostrolateral to the primary visual area and caudal to the primary somatosensory cortex. Overall, this surface callosal projection pattern is similar to what has been shown in flattened cortex (Wang and Burkhalter, 2007). **Figure 5E** shows that overlaying virtual callosal projections with the anatomical template further restrict boundaries of the higher visual areas.

Based on topography and the relationship to callosal projections, individual higher visual areas were drawn from surface views. In **Figure 5**, the lateral visual area located in the caudal part of the large acallosal zone on the lateral side of the primary visual area has a visuotopic map that mirrors the primary visual area. The lateral intermediate area on the lateral side of the lateral visual area and on the caudal side of the anterolateral visual area, which falls in the caudolateral part of the large acallosal zone, has a visuotopic map that mirrors the lateral visual area. The postrhinal area, which falls in the callosally labeled region, has a visuotopic map that mirrors the posterolateral visual area located caudally to the lateral and primary visual areas. The anterolateral visual area, which falls in the rostral part of the large acallosal zone on the rostrolateral side of the primary visual area, has a visuotopic map that mirrors the lateral visual area. The rostrolateral visual area located between the rostrolateral part of the primary visual area and the caudal part of the primary somatosensory area has a visuotopic map that mirrors the anterolateral visual area. The visuotopic map of the anteromedial visual area is a mirror image of the posteromedial visual area.

It is noteworthy that the anterior visual area receives weaker input from the primary visual area compared to other higher visual areas and its visuotopic map is coarse. The boundary of the anterior visual area was drawn between the rostrolateral and the anteromedial visual areas mediolaterally and between the rostral tip of the primary visual areas and the caudal part of the primary somatosensory area rostrocaudally. In total, nine higher visual areas were drawn from the surface views. These 2-D surface drawings were transformed into 3-D by extrapolating surface annotation into the 3-D isocortex by copying the annotation along the streamlines.

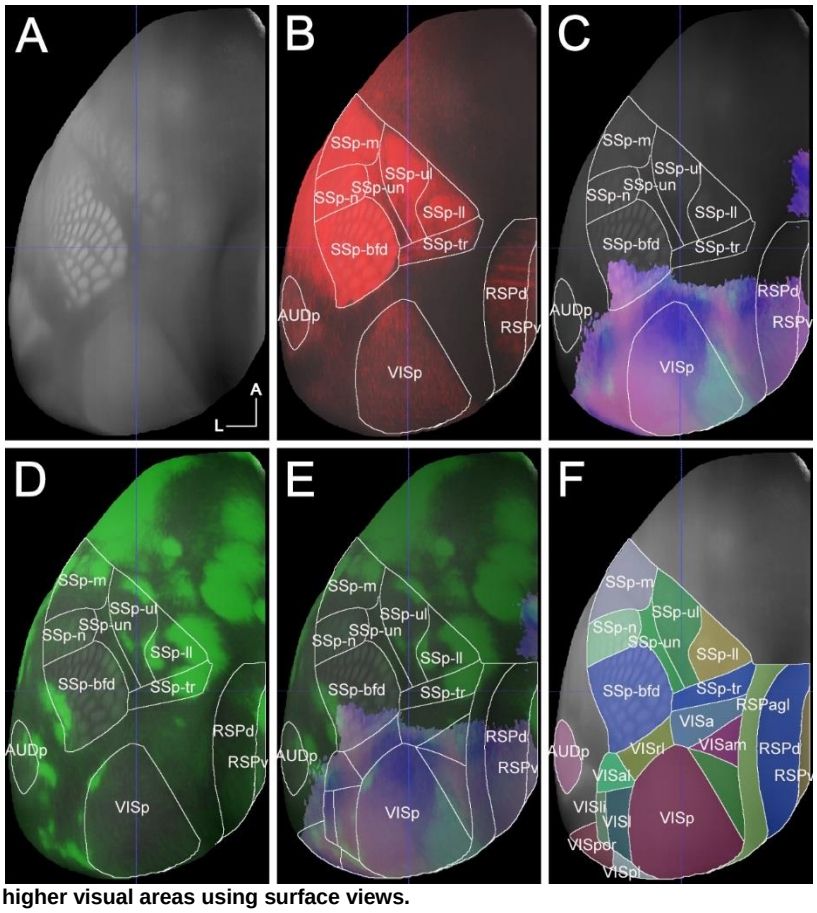

Figure 5. Delineation of higher visual areas using surface views.
A. The anatomical template. **B.** Overlaid image from transgenic line Nr5a1-Cre and SMI-32 stained data set with the anatomical template. **C.** Composite visuotopic maps of striate and extrastriate visual areas. **D.** Virtual callosal projections. **E.** Overlaid visuotopic maps and virtual callosal projections with the anatomical template. **F.** Higher visual areas and their closely-related cortical areas (color coded). Solid lines indicate areal borders. Structure abbreviations listed in **Table 1**. A, anterior; L, lateral.

Remaining Isocortex

Similar to higher visual areas, the remaining isocortex was annotated from seven surface views using the curved cortical coordinate system. All transgenic data used for annotation is listed in **Table 2**. Several examples of these transgenic data are shown in a dorsal view (**Figure 6**) and reveal enriched gene expression patterns in particular isocortical areas. These unique gene expression patterns were used as a guide to delineate isocortex, in addition to those areas readily discernable without any histological staining or immunohistochemical staining in the template itself (**Figure 6A**). These template-distinguishable isocortical areas include the primary visual, primary auditory, primary somatosensory and retrosplenial areas, and are corroborated by gene expression and histological reference data (**Figures 5B**, **6B-H**). This confirmation suggests that the structural data derived from imaging transgenic mice were almost perfectly registered and aligned with the computationally predicted anatomical template in 3-D space. Overlaying the transgenic gene expression data clearly reveals subdivisions of the primary somatosensory area in **Figure 6B** and **6C**. Diminished gene expression signal was found in the retrosplenial area and the primary and secondary motor areas in **Figure 6B-F**. In contrast, enriched gene expression was found in the retrosplenial area (**Figure 6G** and **H**), the primary and secondary motor areas (**Figure 6H-J**), the higher visual areas VISal, VISrl, VISa, VISam and VISpm that belong to the dorsal stream (**Figure 6I**) (Wang *et al*., 2012), and the agranular retrosplenial area (**Figure 6K**). The frontal pole of cerebral cortex was delineated differently between the two mouse brain atlases of Dong (2008) and Paxinos and Franklin (2001). In the Paxinos and Franklin atlas, the frontal association cortex was drawn more than 600 microns along the anterior-posterior axis. In the Dong atlas, however, the frontal pole was drawn in only two plates (200 micron

in the anterior-posterior direction). Physiological recordings performed by Dr. Karel Svoboda's laboratory show that the anterior lateral motor cortex (equivalent to the secondary motor area in the CCF v3) extends extensively into the frontal association cortex indicated by Paxinos and Franklin, indirectly demonstrating that only a small portion of the frontal cortex is possibly devoted to the frontal pole. Here we delineated the frontal pole similar to that in the ARA (**Figure 6L**). Thirty-one of the annotated 43 cortical areas are revealed in the dorsal view (**Figure 6L**). It is important to note that while some gene expression data derived from the transgenic mice reveal some clear cortical areal borders, others do not (**Figure 6**). Therefore, the data from transgenic animals have been used in combination with the projectional data as supporting evidence for structure delineations.

Projectional data (including both cortical and subcortical injections from the Allen Mouse Brain Connectivity Atlas) were used to support delineation of the isocortex in addition to the transgenic data described above. All cortical-relevant injections selected are listed in **Table 3**; a few of which are shown in the top panel of **Figure 7**. Overlaid cortical projections and transgenic expression data are shown with an annotated cortical map in the middle and bottom panels of **Figure 7**, respectively**.** The injection of the primary visual area resulted in projections to ten higher visual areas, including VISal, VISrl, VISa, VISam and VISpm where enriched gene expression is present in Glt25d2 transgenic data (**Figures 6I, 7A, 7E, 7I**). The injection of the anteromedial thalamic nucleus shows weak projections to the higher visual area medial to the primary visual areas and strong projections to the agranular retrosplenial area where enriched gene expression is present in Calb2 transgenic data (**Figures 6K, 7B, 7F, 7J**). The injection of the laterodorsal thalamic nucleus shows strong projections to the retrosplenial area, the higher visual areas including VISal, VISrl, VISa, VISam and VISpm, the barrel fields of the primary somatosensory area and secondary motor area where enriched gene expression is seen in Syt6 transgenic data (**Figures 6H, 7C, 7G, 7K**). Injection primarily into VAL (with secondary infection in VPM) resulted in projections to the primary motor area as well as trunk, lower limb and upper limb subdivisions of the primary somatosensory area. Enriched gene expression in the secondary motor area is complementary to the primary motor area of VAL projections (**Figures 6J, 7D, 7H, 7L**). As demonstrated, connectivity and transgenic data are essential to delineate the isocortex but not without caution. For connectivity, two considerations must be especially accounted for: injection size and spread of infection across multiple areas. Small injections result in projections occupying only a fraction of a given targeted cortical region. On the other hand, injections that result in infection in multiple brain areas can make it difficult to confidently assess the source of labeled axons in a given cortical region. The key to accurate isocortical delineation comes from the integration of multiple lines of evidence. Based on these data sets, a total of 43 cortical areas and their subdivisions were annotated in 3-D space (**Figures 5-7**).

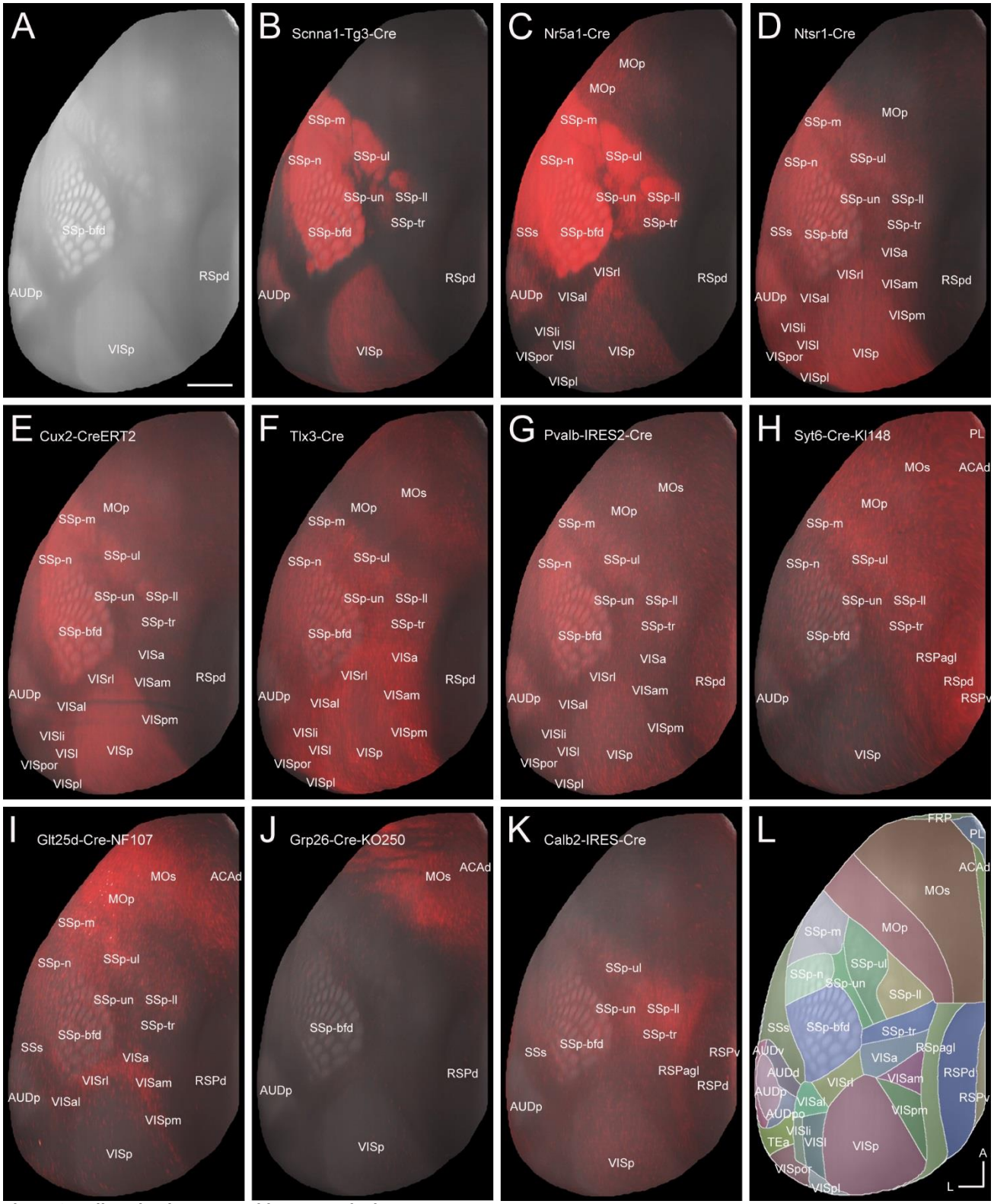

Figure 6. **Delineating isocortex with transgenic data.**
Cortical areas are revealed by overlaying transgenic images with the average template. **A.** A dorsal view of the average template. **B-K**. Dorsal views of the transgenic data show unique and enriched gene expression patterns (red signal) in certain cortical areas and subdivisions. **L.** Delineated cortical area map. Abbreviations are listed in **Table 1**. A, anterior; L, lateral. Scale bar = 1mm.

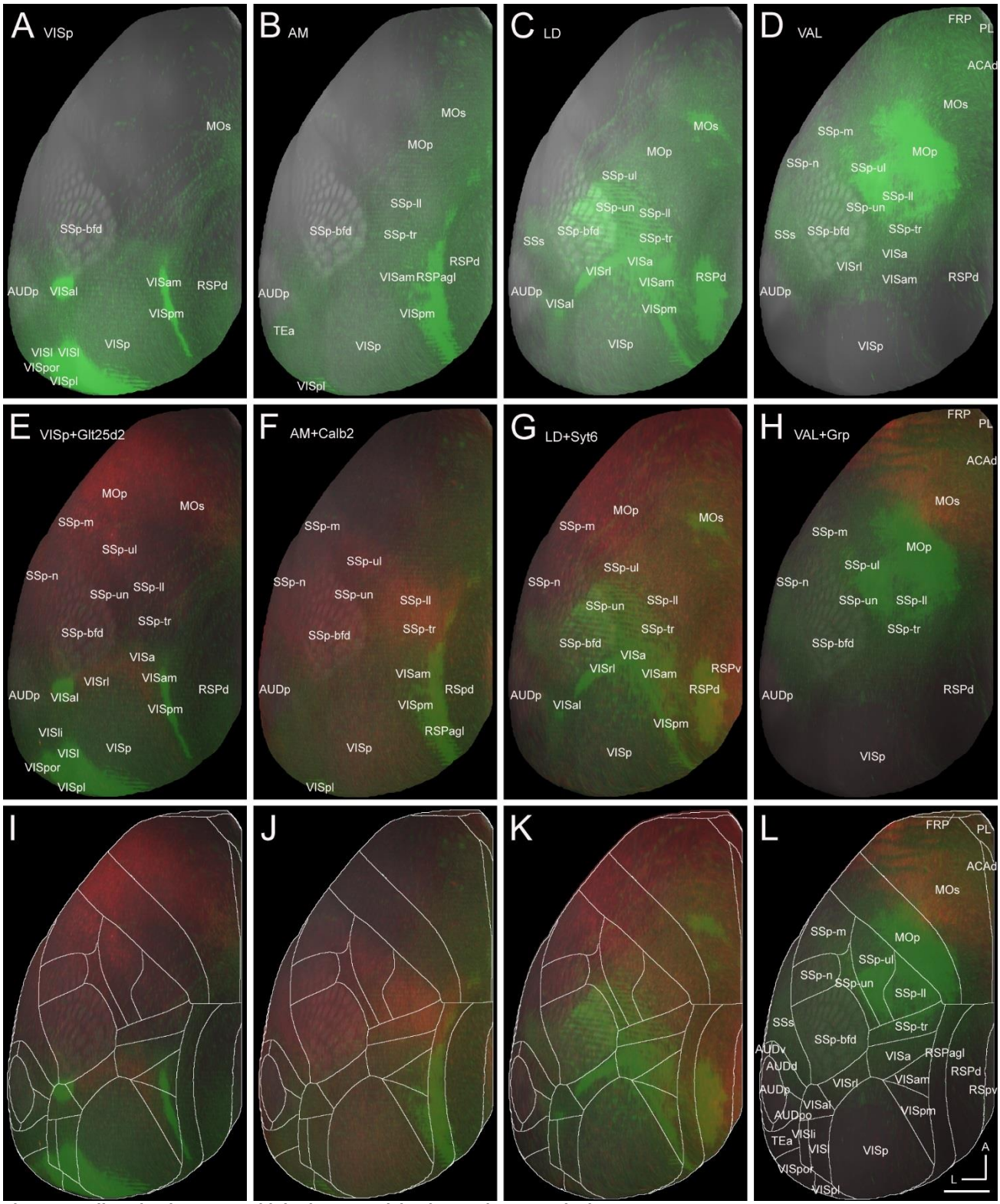

Figure 7. **Delineating isocortex with both connectivity data and transgenic data.**
Cortical areas revealed by overlaying connectivity data and transgenic images with the average template. **A**-**D**. Cortical projections from injections in the primary visual area, and the anteromedial, laterodorsal and ventral anterolateral nuclei of the thalamus (in green). **E**-**H**. Overlay of the connectivity and transgenic data (in red) with the average template. **I**-**L**. Delineated cortical area map. Abbreviations are listed in **Table 1**. L, lateral; A, anterior. Scale bar = 1mm.

Annotation of Isocortical Layers in 3-D Space

Isocortical layers were annotated based on both transgenic data and the anatomical template. Contrast inherent in the anatomical template reveals certain laminar characteristics (**Figure 4B**). Layer 1 is slightly brighter than its border with layer 2/3. Layer 4 is brighter than layers 2/3 and 5, especially in the primary somatosensory, visual and auditory areas. Layer 5 is brighter than layer 6 and is slightly darker at its border with layer 4. This laminar pattern is more apparent in the primary sensory areas than association cortical areas (**Figure 4B**). In addition, transgenic data from transgenic lines with enriched gene expression in one or more layers were selected for delineation of cortical layers. All transgenic data used for delineating cortical layers are listed in **Table 4**. **Figure 8** shows several examples of transgenic data with enriched gene expression in given cortical layer(s): Calb1 (red) for delineating layer 2/3 throughout the isocortex; Nr5a1 (pink), Rorb (purple) and Scnn1a (yellow) for layer 4; Rbp4 (green) for layers 1 and 5; and Ntsr1 (brown) for layers 4 and 6. Ctgf was used to aid in delineating layer 6b (not shown), indicating a 2-3 voxels thickness above white matter. Layers 1, 2/3, 5, 6a, and 6b exist throughout isocortex, while layer 4 is areally limited, lacking presence in orbital, agranular insular, primary and secondary motor, cingulate, retrosplenial, perirhinal and ectorhinal areas. After all cortical layers were reconstructed, they were intersected by all 43 cortical areas, resulting in a total of 242 volumes.

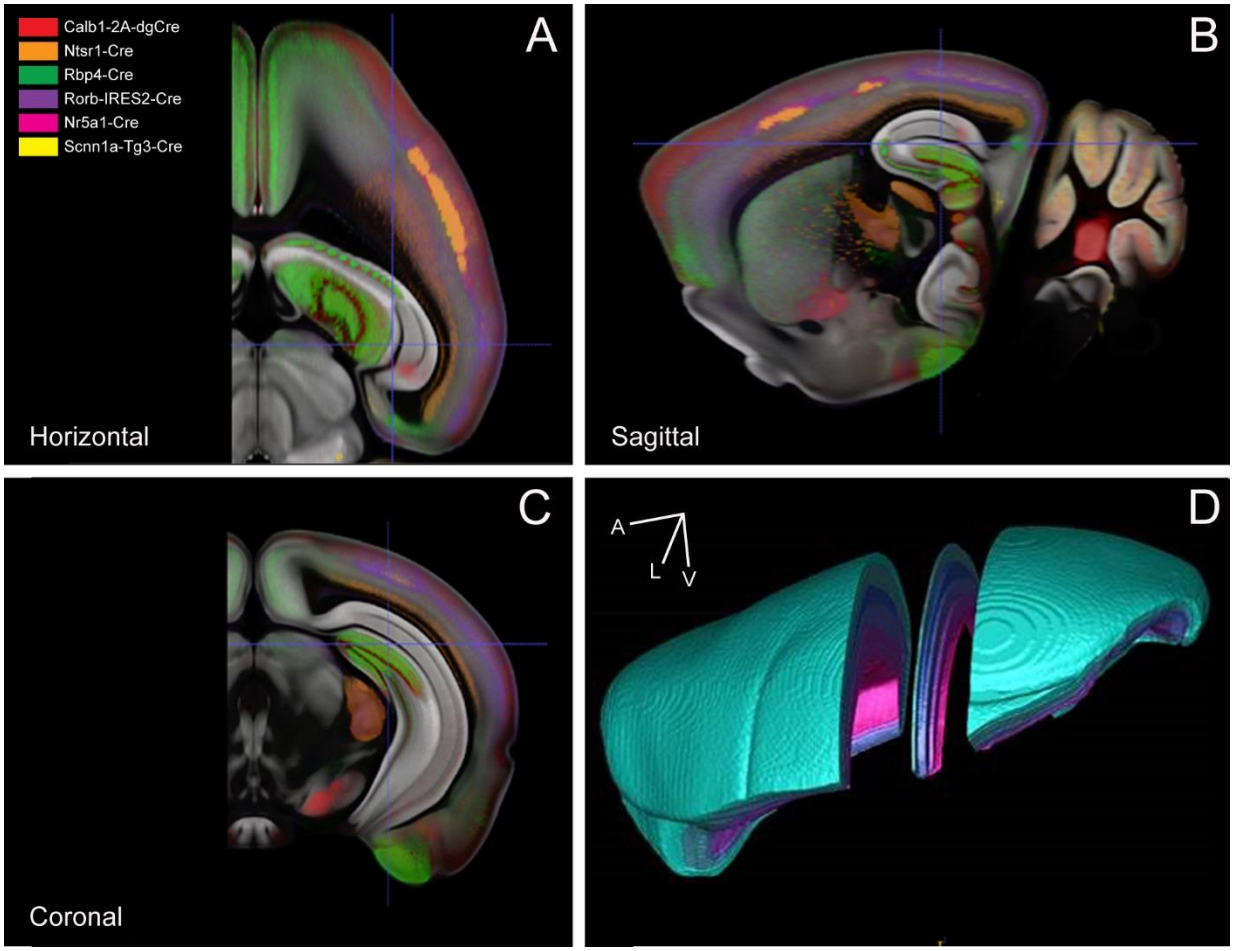

Figure 8. Delineation of isocortical layers in 3-D space.
Isocortical layers were delineated by overlaying the transgenic data with the average template. **A**, **B** and **C**, Horizontal, sagittal and coronal plates, respectively. Each color in the color key represents one transgenic line in **A.** These colors correspond to the false color-coded cortical layers. **D**. Dorsolateral view of cortical layers reconstructed in 3-D space. Each layer is false-color coded in cyan, blue and pink. Abbreviations: A, anterior; L, lateral; V, ventral.

Delineation of Subcortical Structures in 3-D Space

Whereas streamlines were used for delineation of isocortex, subcortical structures were annotated directly in 3-D space after overlaying the histological data, transgenic images and/or connectivity data with the average template. Since the average template was generated based on background signal intensity and shape of 3,350 hemispheres (from 1,675 brains) at 10-micron isotropic resolution, the location, shape, and size of many subcortical structures were revealed in detail and it was used as a primary reference for areal delineations. In general, a subcortical structure containing more and larger cells, such as the anteroventral thalamic nucleus, is brighter (high intensity) than one that contains fewer and smaller cells (low intensity), such as a fiber tract. In addition to the average template, other references were used, such as the transgenic cre driver data with unique enriched gene expression patterns and/or connectivity data with axon terminals in certain subcortical structures. To obtain accurate and smooth structures in 3-D, each subcortical area was annotated through coronal, sagittal, and horizontal planes. Two examples are shown in **Figures 9-10**. **Figure 9** shows delineation of the dorsal part of the lateral geniculate nucleus (LGd), a thalamic relay nucleus from retina to the primary visual cortex, subdivided into three regions: shell, core, and ipsilateral zones (**Figure 9M-O**). LGd was not previously subdivided in widely used atlases (e.g. ARA and Paxinos and Franklin's mouse atlas). Here, by overlaying transgenic cre driver data and retinal axon projection data (connectivity data) with the average template, the subdivisions were visible. The shell, at the dorsolateral surface of the LGd, contains dense gene expression in the Calb2-IRES-Cre line (**Figure 9A-C**). It also receives denser axonal projections compared to the core and ipsilateral zones from retinal ganglion cells (RGCs) labeled in the Cart-Tg1-Cre mouse line (**Figure9D-F**). In contrast, the core region, at the ventromedial part of the LGd, receives denser axon projections as compared to the shell and ipsilateral zone from RGCs labeled in the Kcng4-Cre line (**Figure 9G-H**). The ipsilateral zone receives little to no input from RGCs labeled in the ipsilateral retina of the Chrna2-Cre-OE25 line, but is surrounded by axon terminals distributed in the shell and core (**Figure 9J-L**).

Another example of subcortical structure delineation is the claustrum (CLA), located between the striatum and the agranular insular cortex. The CLA was drawn as a larger structure in both the ARA and Paxinos and Franklin's mouse atlas. In our recent study (Wang et al., 2016) the CLA was delineated based on the average template, transgenic cre driver and connectivity data. In the average template, the CLA is brighter than its surrounding structures (**Figure 10A-C**) and shows enriched Cux2 gene expression in the Cux2-CreERT2 mouse line, but a lack of Ctgf gene expression in the Ctgf-2A-dgCre mouse line (**Figure 10D-F**). The CLA receives strong input from the infralimbic area, whereas its neighboring endopiriform nucleus receives less input (**Figure 10G-I**). This elongated structure across the anteroposterior axis is narrow in its mediolateral extent, starting as relatively large anteriorly, and becoming gradually smaller toward the posterior end (**Figure 10J-L**).

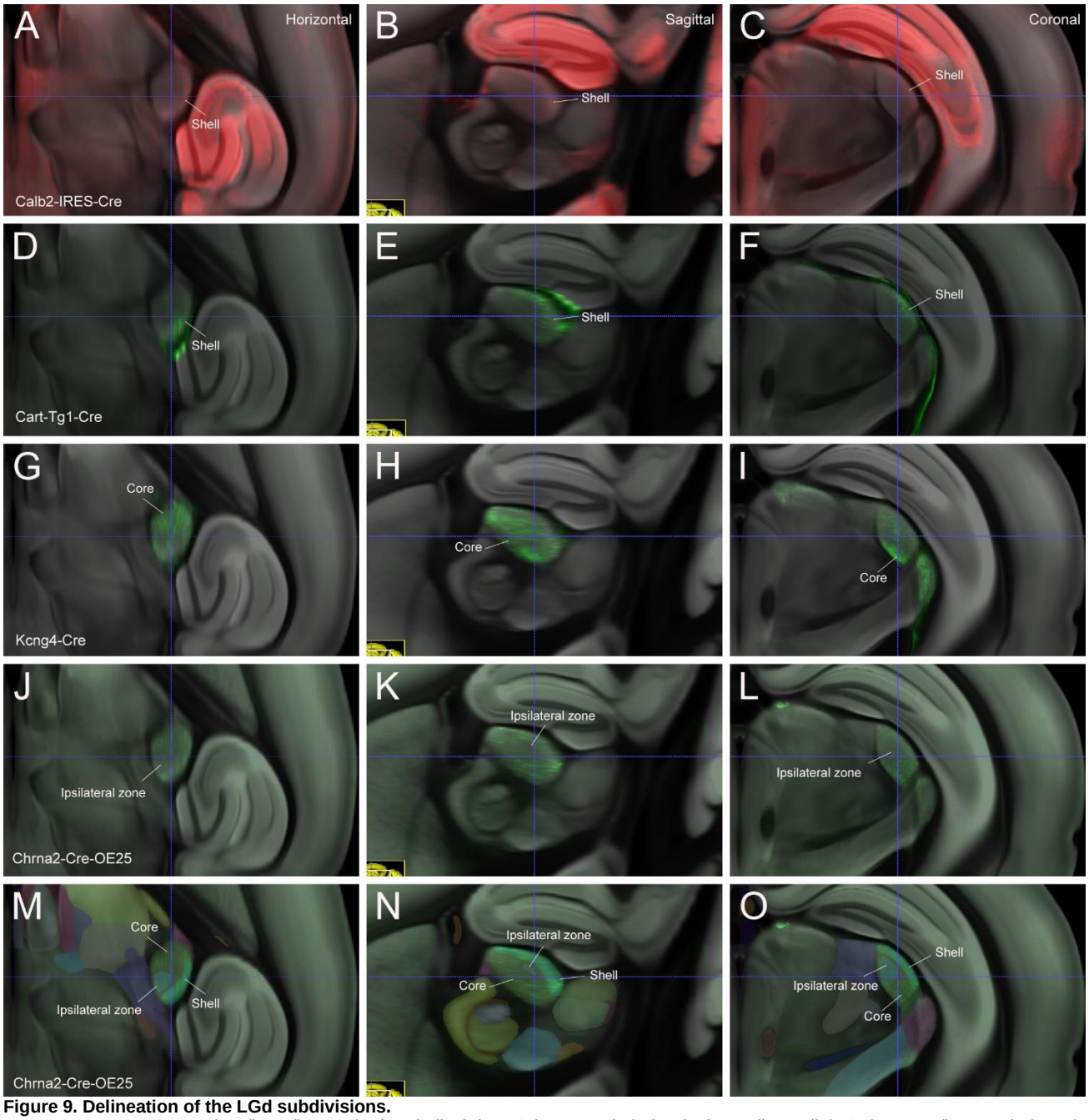

Figure 9. Delineation of the LGd subdivisions.
A-C, Dense gene expression (in red) reveals the shell of the LGd. **D-F**, Labeled retinal ganglion cell (RGC) axons (in green) densely innervate the LGd shell. **G-I**, Labeled RGC axons terminate densely in the LGd core. **J-L**, RGC axons avoid the ipsilateral zone but terminate in the shell and core. **M-O**, The shell, core and ipsilateral zone are color-coded differently to indicate their final positions in the LGd. Shell, core and ipsilateral zones are shown in horizontal (**A, D, G, J, M**), sagittal (**B, E, H, K, N**) and coronal planes (**C, F, I, L, O**).

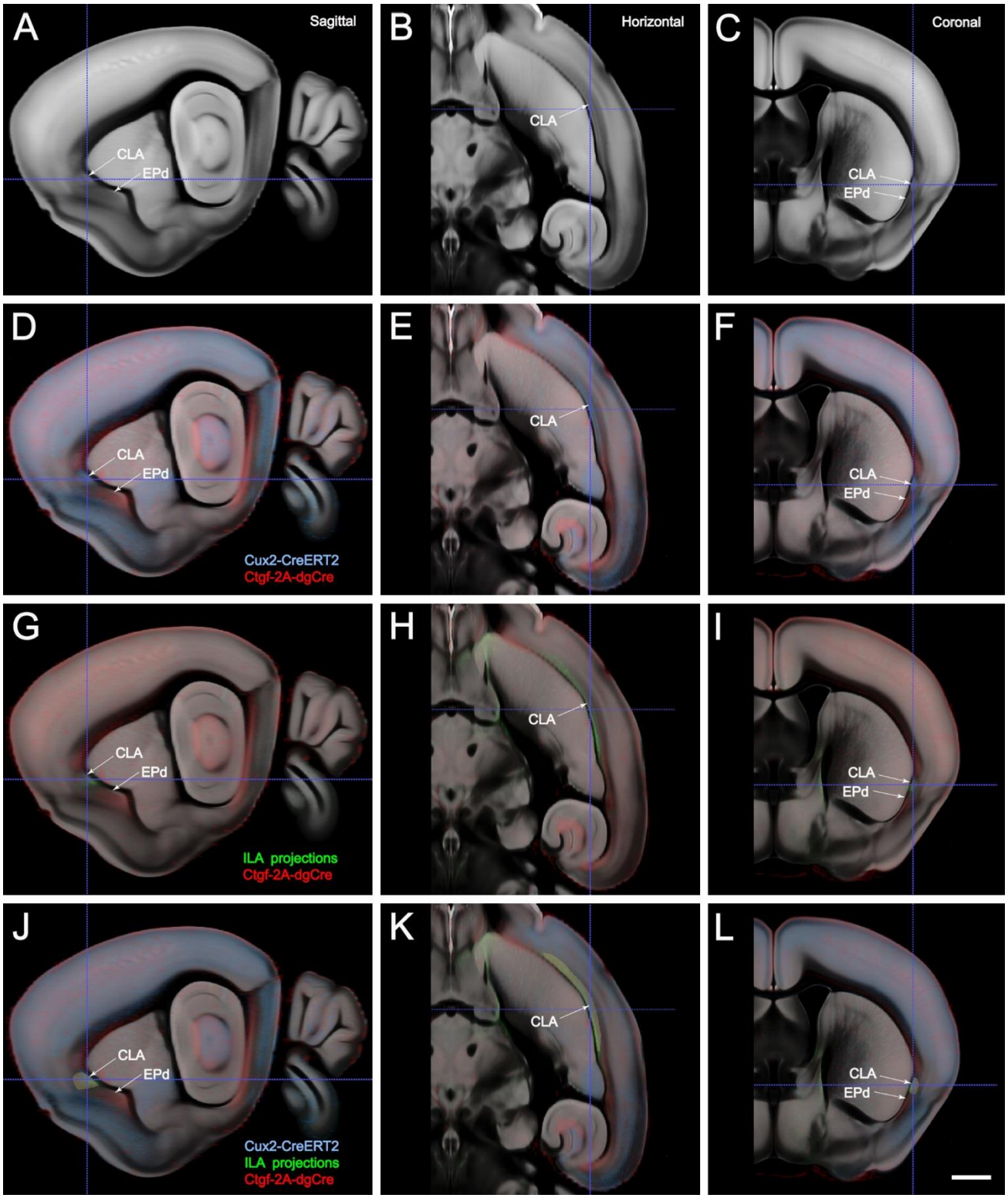

Figure 10. Delineation of the claustrum.
A-C, In the average template, the claustrum is brighter than its immediate surroundings. **D-F**, The claustrum has enriched Cux2-CreERT2 gene expression (in cyan) but is lacking Ctgf-2A-dgCre gene expression (in red). **G-I**, The claustrum receives strong projections from the infralimbic cortex (in green) but less in endopiriform nucleus (EPd), which has enriched Ctgf-2A-dgCre gene expression (in red). **J-L**, The claustrum is color-coded in light green in sagittal, horizontal and coronal sections. Arrows indicate the claustrum and endopiriform nucleus in sagittal (**A, D, G, J**), horizontal (**B, E, H, K**) and coronal planes (**C, F, I, L**).

White Matter Tracts and Ventricles

The delineation of white matter (WM) tracts was made based on inherent contrast features in the anatomical template in combination with myelin basic protein (SMI-99), neurofilaments (SMI-32 and NF-160), parvalbumin (PV), and calbindin (CB) reference stains. Although WM tracts generally exhibited lower signal intensity (darker) than gray matter structures (brighter) in the anatomical template, these features were not necessarily homogenous between different WM tracts or along individual WM tracts themselves. In the case of isolated and solid WM bundles such as anterior commissure, fornix, fasciculus retroflexus, and mammilothalamic tract, contours and trajectories were easily defined without the need of additional data.

In most other cases, however, WM tracts adjoined, merged (mix) or intersected other bundles and/or portions of gray matter structures at particular locations, leading to complex signal intensities along their paths, thus necessitating the correlation of template signal intensity with reference data for accurate delineation of boundaries and trajectories. For example, the medial lemniscus travels through the medulla, pons, and midbrain on its way to the thalamus, exhibiting significant changes in shape, size, location, topography, and signal intensity throughout (**Figure 11**). Specifically, intermediate intensity (medium-dark) was seen in the thalamus (**Figure 11A**) and upper midbrain (**Figure 11B**), low intensity (dark) was seen in the lower midbrain (**Figure 11C**), high intensity (least dark) in the upper pons (**Figure 11D**), and low intensity (dark) in the lower pons (**Figure 11E**) and medulla (**Figure 11F**). The trajectory and contour of the medial lemniscus was confirmed by analysis of sequential PV-stained sections, which revealed strong staining and a distinct fiber orientation pattern (green in **Figure 11A'- 11F'**). It is important to note that the medial lemniscus adjoins the cerebral peduncle (cpd) in the lower midbrain (**Figure 11C**), mixes in the upper pons with other fibers, which are PV-negative and SMI-32 positive (red in **Figure 11D**), and is crossed in the lower pons by the trapezoid body (tb), which is PV-positive but runs in a transverse direction (green in **Figure 11E**). In the medulla, the medial lemniscus is located dorsal to the pyramidal tract (py), which is negative in both PV and SMI-32 stains (**Figure 11F**).

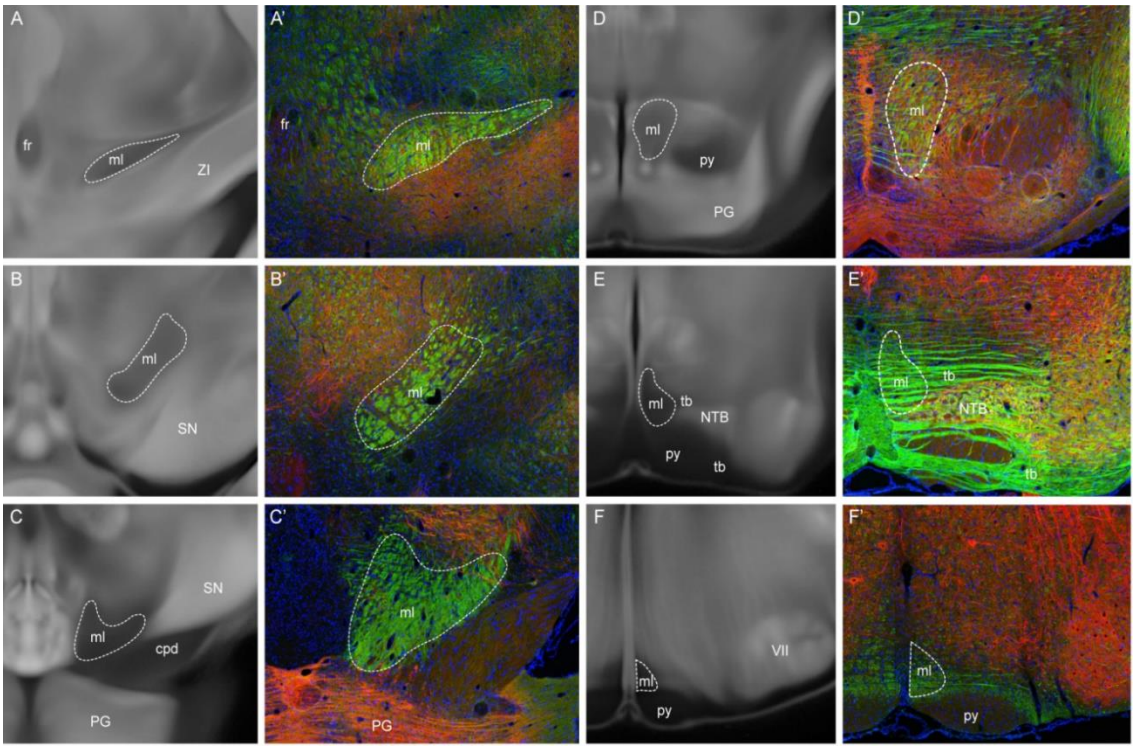

Figure 11. Changes in location, shape, size, topography and signal intensity of the medial lemniscus (ml) along its trajectory and the usefulness of reference data in delineation of white matter tracts.
A-F. Rostral–caudal template images containing the medial lemniscus and adjoining structures. **A'-F'.** Double-stained sections at the levels **A-F** showing PV- (green) and SMI-32- (red) stained gray and white matter structures. These sections were also counterstained with DAPI (blue). Abbreviations: ZI, zona incerta; fr, fasciculus retroflexus; SN, substantia nigra; cpd, cerebral peduncle; PG, pontine gray; py, pyramid; tb, trapezoid body; NTB, nucleus of the trapezoid body; VII, facial motor nucleus.

In certain cases, other stains were used, as were tracer experiments from the Allen Mouse Brain Connectivity Atlas. Allen Mouse Brain Connectivity Atlas data (Oh *et al*., 2014) was especially useful when the anterograde tracer (rAAV) was injected in a desired anatomic structure restrictively (*e.g.* red nucleus). In this scenario, trajectories of a fiber bundle (*e.g.* rubrospinal tract originated from red nucleus) were confidently traced with modest adjustment according to contours exhibited in other reference data.

Finally, the ventricular system (lateral, third, fourth ventricles and cerebral aqueduct and central canal) was also delineated based on low signal intensity (dark) with exception in the regions occupied by the choroid plexus, which display higher signal intensity (less dark) and were included in the corresponding ventricles. The ependymal layer lining all the ventricular walls were also included in the corresponding ventricles.

Table 1. Anatomical structures delineated in 3-D for the CCF
Newly added structures are shaded.

Name	Acronym	Parent Brain Region
Frontal pole, layer 1	FRP1	Isocortex
Frontal pole, layer 2/3	FRP2/3	Isocortex
Frontal pole, layer 5	FRP5	Isocortex
Frontal pole, layer 6a	FRP6a	Isocortex
Frontal pole, layer 6b	FRP6b	Isocortex
Primary motor area, Layer 1	MOp1	Isocortex
Primary motor area, Layer 2/3	MOp2/3	Isocortex
Primary motor area, Layer 5	MOp5	Isocortex
Primary motor area, Layer 6a	MOp6a	Isocortex
Primary motor area, Layer 6b	MOp6b	Isocortex
Secondary motor area, layer 1	MOs1	Isocortex
Secondary motor area, layer 2/3	MOs2/3	Isocortex
Secondary motor area, layer 5	MOs5	Isocortex
Secondary motor area, layer 6a	MOs6a	Isocortex
Secondary motor area, layer 6b	MOs6b	Isocortex
Primary somatosensory area, nose, layer 1	SSp-n1	Isocortex
Primary somatosensory area, nose, layer 2/3	SSp-n2/3	Isocortex
Primary somatosensory area, barrel field, layer 4	SSp-n4	Isocortex
Primary somatosensory area, barrel field, layer 5	SSp-n5	Isocortex
Primary somatosensory area, barrel field, layer 6a	SSp-n6a	Isocortex
Primary somatosensory area, barrel field, layer 6b	SSp-n6b	Isocortex
Primary somatosensory area, barrel field, layer 1	SSp-bfd1	Isocortex
Primary somatosensory area, barrel field, layer 2/3	SSp-bfd2/3	Isocortex
Primary somatosensory area, barrel field, layer 4	SSp-bfd4	Isocortex
Primary somatosensory area, barrel field, layer 5	SSp-bfd5	Isocortex
Primary somatosensory area, barrel field, layer 6a	SSp-bfd6a	Isocortex
Primary somatosensory area, barrel field, layer 6b	SSp-bfd6b	Isocortex
Primary somatosensory area, lower limb, layer 1	SSp-ll1	Isocortex
Primary somatosensory area, lower limb, layer 2/3	SSp-ll2/3	Isocortex
Primary somatosensory area, lower limb, layer 4	SSp-ll4	Isocortex
Primary somatosensory area, lower limb, layer 5	SSp-ll5	Isocortex
Primary somatosensory area, lower limb, layer 6a	SSp-ll6a	Isocortex
Primary somatosensory area, lower limb, layer 6b	SSp-ll6b	Isocortex
Primary somatosensory area, mouth, layer 1	SSp-m1	Isocortex
Primary somatosensory area, mouth, layer 2/3	SSp-m2/3	Isocortex
Primary somatosensory area, mouth, layer 4	SSp-m4	Isocortex
Primary somatosensory area, mouth, layer 5	SSp-m5	Isocortex
Primary somatosensory area, mouth, layer 6a	SSp-m6a	Isocortex
Primary somatosensory area, mouth, layer 6b	SSp-m6b	Isocortex
Primary somatosensory area, upper limb, layer 1	SSp-ul1	Isocortex
Primary somatosensory area, upper limb, layer 2/3	SSp-ul2/3	Isocortex
Primary somatosensory area, upper limb, layer 4	SSp-ul4	Isocortex
Primary somatosensory area, upper limb, layer 5	SSp-ul5	Isocortex
Primary somatosensory area, upper limb, layer 6a	SSp-ul6a	Isocortex
Primary somatosensory area, upper limb, layer 6b	SSp-ul6b	Isocortex
Primary somatosensory area, trunk, layer 1	SSp-tr1	Isocortex
Primary somatosensory area, trunk, layer 2/3	SSp-tr2/3	Isocortex
Primary somatosensory area, trunk, layer 4	SSp-tr4	Isocortex
Primary somatosensory area, trunk, layer 5	SSp-tr5	Isocortex
Primary somatosensory area, trunk, layer 6a	SSp-tr6a	Isocortex
Primary somatosensory area, trunk, layer 6b	SSp-tr6b	Isocortex

Primary somatosensory area, unassigned, layer 1	SSp-un1	Isocortex
Primary somatosensory area, unassigned, layer 2/3	SSp-un2/3	Isocortex
Primary somatosensory area, unassigned, layer 4	SSp-un4	Isocortex
Primary somatosensory area, unassigned, layer 5	SSp-un5	Isocortex
Primary somatosensory area, unassigned, layer 6a	SSp-un6a	Isocortex
Primary somatosensory area, unassigned, layer 6b	SSp-un6b	Isocortex
Supplemental somatosensory area, layer 1	SSs1	Isocortex
Supplemental somatosensory area, layer 2/3	SSs2/3	Isocortex
Supplemental somatosensory area, layer 4	SSs4	Isocortex
Supplemental somatosensory area, layer 5	SSs5	Isocortex
Supplemental somatosensory area, layer 6a	SSs6a	Isocortex
Supplemental somatosensory area, layer 6b	SSs6b	Isocortex
Gustatory areas, layer 1	GU1	Isocortex
Gustatory areas, layer 2/3	GU2/3	Isocortex
Gustatory areas, layer 4	GU4	Isocortex
Gustatory areas, layer 5	GU5	Isocortex
Gustatory areas, layer 6a	GU6a	Isocortex
Gustatory areas, layer 6b	GU6b	Isocortex
Visceral area, layer 1	VISC1	Isocortex
Visceral area, layer 2/3	VISC2/3	Isocortex
Visceral area, layer 4	VISC4	Isocortex
Visceral area, layer 5	VISC5	Isocortex
Visceral area, layer 6a	VISC6a	Isocortex
Visceral area, layer 6b	VISC6b	Isocortex
Dorsal auditory area, layer 1	AUDd1	Isocortex
Dorsal auditory area, layer 2/3	AUDd2/3	Isocortex
Dorsal auditory area, layer 4	AUDd4	Isocortex
Dorsal auditory area, layer 5	AUDd5	Isocortex
Dorsal auditory area, layer 6a	AUDd6a	Isocortex
Dorsal auditory area, layer 6b	AUDd6b	Isocortex
Primary auditory area, layer 1	AUDp1	Isocortex
Primary auditory area, layer 2/3	AUDp2/3	Isocortex
Primary auditory area, layer 4	AUDp4	Isocortex
Primary auditory area, layer 5	AUDp5	Isocortex
Primary auditory area, layer 6a	AUDp6a	Isocortex
Primary auditory area, layer 6b	AUDp6b	Isocortex
Posterior auditory area, layer 1	AUDpo1	Isocortex
Posterior auditory area, layer 2/3	AUDpo2/3	Isocortex
Posterior auditory area, layer 4	AUDpo4	Isocortex
Posterior auditory area, layer 5	AUDpo5	Isocortex
Posterior auditory area, layer 6a	AUDpo6a	Isocortex
Posterior auditory area, layer 6b	AUDpo6b	Isocortex
Ventral auditory area, layer 1	AUDv1	Isocortex
Ventral auditory area, layer 2/3	AUDv2/3	Isocortex
Ventral auditory area, layer 4	AUDv4	Isocortex
Ventral auditory area, layer 5	AUDv5	Isocortex
Ventral auditory area, layer 6a	AUDv6a	Isocortex
Ventral auditory area, layer 6b	AUDv6b	Isocortex
Anterolateral visual area, layer 1	VISal1	Isocortex
Anterolateral visual area, layer 2/3	VISal2/3	Isocortex
Anterolateral visual area, layer 4	VISal4	Isocortex
Anterolateral visual area, layer 5	VISal5	Isocortex
Anterolateral visual area, layer 6a	VISal6a	Isocortex
Anterolateral visual area, layer 6b	VISal6b	Isocortex

Anteromedial visual area, layer 1	VISam1	Isocortex
Anteromedial visual area, layer 2/3	VISam2/3	Isocortex
Anteromedial visual area, layer 4	VISam4	Isocortex
Anteromedial visual area, layer 5	VISam5	Isocortex
Anteromedial visual area, layer 6a	VISam6a	Isocortex
Anteromedial visual area, layer 6b	VISam6b	Isocortex
Lateral visual area, layer 1	VISl1	Isocortex
Lateral visual area, layer 2/3	VISl2/3	Isocortex
Lateral visual area, layer 4	VISl4	Isocortex
Lateral visual area, layer 5	VISl5	Isocortex
Lateral visual area, layer 6a	VISl6a	Isocortex
Lateral visual area, layer 6b	VISl6b	Isocortex
Primary visual area, layer 1	VISp1	Isocortex
Primary visual area, layer 2/3	VISp2/3	Isocortex
Primary visual area, layer 4	VISp4	Isocortex
Primary visual area, layer 5	VISp5	Isocortex
Primary visual area, layer 6a	VISp6a	Isocortex
Primary visual area, layer 6b	VISp6b	Isocortex
Posterolateral visual area, layer 1	VISpl1	Isocortex
Posterolateral visual area, layer 2/3	VISpl2/3	Isocortex
Posterolateral visual area, layer 4	VISpl4	Isocortex
Posterolateral visual area, layer 5	VISpl5	Isocortex
Posterolateral visual area, layer 6a	VISpl6a	Isocortex
Posterolateral visual area, layer 6b	VISpl6b	Isocortex
posteromedial visual area, layer 1	VISpm1	Isocortex
posteromedial visual area, layer 2/3	VISpm2/3	Isocortex
posteromedial visual area, layer 4	VISpm4	Isocortex
posteromedial visual area, layer 5	VISpm5	Isocortex
posteromedial visual area, layer 6a	VISpm6a	Isocortex
posteromedial visual area, layer 6b	VISpm6b	Isocortex
Laterointermediate area, layer 1	VISli1	Isocortex
Laterointermediate area, layer 2/3	VISli2/3	Isocortex
Laterointermediate area, layer 4	VISli4	Isocortex
Laterointermediate area, layer 5	VISli5	Isocortex
Laterointermediate area, layer 6a	VISli6a	Isocortex
Laterointermediate area, layer 6b	VISli6b	Isocortex
Postrhinal area, layer 1	VISpor1	Isocortex
Postrhinal area, layer 2/3	VISpor2/3	Isocortex
Postrhinal area, layer 4	VISpor4	Isocortex
Postrhinal area, layer 5	VISpor5	Isocortex
Postrhinal area, layer 6a	VISpor6a	Isocortex
Postrhinal area, layer 6b	VISpor6b	Isocortex
Anterior cingulate area, dorsal part, layer 1	ACAd1	Isocortex
Anterior cingulate area, dorsal part, layer 2/3	ACAd2/3	Isocortex
Anterior cingulate area, dorsal part, layer 5	ACAd5	Isocortex
Anterior cingulate area, dorsal part, layer 6a	ACAd6a	Isocortex
Anterior cingulate area, dorsal part, layer 6b	ACAd6b	Isocortex
Anterior cingulate area, ventral part, layer 1	ACAv1	Isocortex
Anterior cingulate area, ventral part, layer 2/3	ACAv2/3	Isocortex
Anterior cingulate area, ventral part, layer 5	ACAv5	Isocortex
Anterior cingulate area, ventral part, 6a	ACAv6a	Isocortex
Anterior cingulate area, ventral part, 6b	ACAv6b	Isocortex
Prelimbic area, layer 1	PL1	Isocortex
Prelimbic area, layer 2/3	PL2/3	Isocortex

Prelimbic area, layer 5	PL5	Isocortex
Prelimbic area, layer 6a	PL6a	Isocortex
Prelimbic area, layer 6b	PL6b	Isocortex
Infralimbic area, layer 1	ILA1	Isocortex
Infralimbic area, layer 2/3	ILA2/3	Isocortex
Infralimbic area, layer 5	ILA5	Isocortex
Infralimbic area, layer 6a	ILA6a	Isocortex
Infralimbic area, layer 6b	ILA6b	Isocortex
Orbital area, lateral part, layer 1	ORBl1	Isocortex
Orbital area, lateral part, layer 2/3	ORBl2/3	Isocortex
Orbital area, lateral part, layer 5	ORBl5	Isocortex
Orbital area, lateral part, layer 6a	ORBl6a	Isocortex
Orbital area, lateral part, layer 6b	ORBl6b	Isocortex
Orbital area, medial part, layer 1	ORBm1	Isocortex
Orbital area, medial part, layer 2/3	ORBm2/3	Isocortex
Orbital area, medial part, layer 5	ORBm5	Isocortex
Orbital area, medial part, layer 6a	ORBm6a	Isocortex
Orbital area, medial part, layer 6b	ORBm6b	Isocortex
Orbital area, ventrolateral part, layer 1	ORBvl1	Isocortex
Orbital area, ventrolateral part, layer 2/3	ORBvl2/3	Isocortex
Orbital area, ventrolateral part, layer 5	ORBvl5	Isocortex
Orbital area, ventrolateral part, layer 6a	ORBvl6a	Isocortex
Orbital area, ventrolateral part, layer 6b	ORBvl6b	Isocortex
Agranular insular area, dorsal part, layer 1	AId1	Isocortex
Agranular insular area, dorsal part, layer 2/3	AId2/3	Isocortex
Agranular insular area, dorsal part, layer 5	AId5	Isocortex
Agranular insular area, dorsal part, layer 6a	AId6a	Isocortex
Agranular insular area, dorsal part, layer 6b	AId6b	Isocortex
Agranular insular area, posterior part, layer 1	AIp1	Isocortex
Agranular insular area, posterior part, layer 2/3	AIp2/3	Isocortex
Agranular insular area, posterior part, layer 5	AIp5	Isocortex
Agranular insular area, posterior part, layer 6a	AIp6a	Isocortex
Agranular insular area, posterior part, layer 6b	AIp6b	Isocortex
Agranular insular area, ventral part, layer 1	AIv1	Isocortex
Agranular insular area, ventral part, layer 2/3	AIv2/3	Isocortex
Agranular insular area, ventral part, layer 5	AIv5	Isocortex
Agranular insular area, ventral part, layer 6a	AIv6a	Isocortex
Agranular insular area, ventral part, layer 6b	AIv6b	Isocortex
Retrosplenial area, lateral agranular part, layer 1	RSPagl1	Isocortex
Retrosplenial area, lateral agranular part, layer 2/3	RSPagl2/3	Isocortex
Retrosplenial area, lateral agranular part, layer 4	RSPagl4	Isocortex
Retrosplenial area, lateral agranular part, layer 5	RSPagl5	Isocortex
Retrosplenial area, lateral agranular part, layer 6a	RSPagl6a	Isocortex
Retrosplenial area, lateral agranular part, layer 6b	RSPagl6b	Isocortex
Retrosplenial area, dorsal part, layer 1	RSPd1	Isocortex
Retrosplenial area, dorsal part, layer 2/3	RSPd2/3	Isocortex
Retrosplenial area, dorsal part, layer 4	RSPd4	Isocortex
Retrosplenial area, dorsal part, layer 5	RSPd5	Isocortex
Retrosplenial area, dorsal part, layer 6a	RSPd6a	Isocortex
Retrosplenial area, dorsal part, layer 6b	RSPd6b	Isocortex
Retrosplenial area, ventral part, layer 1	RSPv1	Isocortex
Retrosplenial area, ventral part, layer 2/3	RSPv2/3	Isocortex
Retrosplenial area, ventral part, layer 5	RSPv5	Isocortex
Retrosplenial area, ventral part, layer 6a	RSPv6a	Isocortex

Retrosplenial area, ventral part, layer 6b	RSPv6b	Isocortex
Anterior area, layer 1	VISa1	Isocortex
Anterior area, layer 2/3	VISa2/3	Isocortex
Anterior area, layer 4	VISa4	Isocortex
Anterior area, layer 5	VISa5	Isocortex
Anterior area, layer 6a	VISa6a	Isocortex
Anterior area, layer 6b	VISa6b	Isocortex
Rostrolateral area, layer 1	VISrl1	Isocortex
Rostrolateral area, layer 2/3	VISrl2/3	Isocortex
Rostrolateral area, layer 4	VISrl4	Isocortex
Rostrolateral area, layer 5	VISrl5	Isocortex
Rostrolateral area, layer 6a	VISrl6a	Isocortex
Rostrolateral area, layer 6b	VISrl6b	Isocortex
Temporal association areas, layer 1	TEa1	Isocortex
Temporal association areas, layer 2/3	TEa2/3	Isocortex
Temporal association areas, layer 4	TEa4	Isocortex
Temporal association areas, layer 5	TEa5	Isocortex
Temporal association areas, layer 6a	TEa6a	Isocortex
Temporal association areas, layer 6b	TEa6b	Isocortex
Perirhinal area, layer 6a	PERI6a	Isocortex
Perirhinal area, layer 6b	PERI6b	Isocortex
Perirhinal area, layer 1	PERI1	Isocortex
Perirhinal area, layer 5	PERI5	Isocortex
Perirhinal area, layer 2/3	PERI2/3	Isocortex
Ectorhinal area/Layer 1	ECT1	Isocortex
Ectorhinal area/Layer 2/3	ECT2/3	Isocortex
Ectorhinal area/Layer 5	ECT5	Isocortex
Ectorhinal area/Layer 6a	ECT6a	Isocortex
Ectorhinal area/Layer 6b	ECT6b	Isocortex
Main olfactory bulb	MOB	Olfactory areas
Accessory olfactory bulb, glomerular layer	AOBgl	Olfactory areas
Accessory olfactory bulb, granular layer	AOBgr	Olfactory areas
Accessory olfactory bulb, mitral layer	AOBmi	Olfactory areas
Anterior olfactory nucleus	AON	Olfactory areas
Taenia tecta, dorsal part	TTd	Olfactory areas
Taenia tecta, ventral part	TTv	Olfactory areas
Dorsal peduncular area	DP	Olfactory areas
Piriform area	PIR	Olfactory areas
Nucleus of the lateral olfactory tract, molecular layer	NLOT1	Olfactory areas
Nucleus of the lateral olfactory tract, pyramidal layer	NLOT2	Olfactory areas
Nucleus of the lateral olfactory tract, layer 3	NLOT3	Olfactory areas
Cortical amygdalar area, anterior part	COAa	Olfactory areas
Cortical amygdalar area, posterior part, lateral zone	COApl	Olfactory areas
Cortical amygdalar area, posterior part, medial zone	COApm	Olfactory areas
Piriform-amygdalar area	PAA	Olfactory areas
Postpiriform transition area	TR	Olfactory areas
Field CA1	CA1	Hippocapal formation
Field CA2	CA2	Hippocapal formation
Field CA3	CA3	Hippocapal formation
Dentate gyrus, molecular layer	DG-mo	Hippocapal formation
Dentate gyrus, polymorph layer	DG-po	Hippocapal formation
Dentate gyrus, granule cell layer	DG-sg	Hippocapal formation
Fasciola cinerea	FC	Hippocapal formation
Induseum griseum	IG	Hippocapal formation

Entorhinal area, lateral part, layer 1	ENTl1	Hippocapal formation
Entorhinal area, lateral part, layer 2	ENTl2	Hippocapal formation
Entorhinal area, lateral part, layer 3	ENTl3	Hippocapal formation
Entorhinal area, lateral part, layer 5	ENTl5	Hippocapal formation
Entorhinal area, lateral part, layer 6a	ENTl6a	Hippocapal formation
Entorhinal area, medial part, dorsal zone, layer 1	ENTm1	Hippocapal formation
Entorhinal area, medial part, dorsal zone, layer 2	ENTm2	Hippocapal formation
Entorhinal area, medial part, dorsal zone, layer 3	ENTm3	Hippocapal formation
Entorhinal area, medial part, dorsal zone, layer 5	ENTm5	Hippocapal formation
Entorhinal area, medial part, dorsal zone, layer 6	ENTm6	Hippocapal formation
Parasubiculum	PAR	Hippocapal formation
Postsubiculum	POST	Hippocapal formation
Presubiculum	PRE	Hippocapal formation
Subiculum	SUB	Hippocapal formation
Prosubiculum	ProS	Hippocapal formation
Hippocampo-amygdalar transition area	HATA	Hippocapal formation
Area prostriata	APr	Hippocapal formation
Claustrum	CLA	Cortical subplate
Endopiriform nucleus, dorsal part	EPd	Cortical subplate
Endopiriform nucleus, ventral part	EPv	Cortical subplate
Lateral Amygdalar nucleus	LA	Cortical subplate
Basolateral amygdalar nucleus, anterior part	BLAa	Cortical subplate
Basolateral amygdalar nucleus, posterior part	BLAp	Cortical subplate
Basolateral amygdalar nucleus, ventral part	BLAv	Cortical subplate
Basomedial amygdalar nucleus, anterior part	BMAa	Cortical subplate
Basomedial amygdalar nucleus, posterior part	BMAp	Cortical subplate
Posterior amygdalar nucleus	PA	Cortical subplate
Caudoputamen	CP	Striatum
Nucleus accumbens	ACB	Striatum
Fundus of striatum	FS	Striatum
Olfactory tubercle	OT	Striatum
Lateral septal nucleus, caudal (caudodorsal) part	LSc	Striatum
Lateral septal nucleus, rostral (rostroventral) part	LSr	Striatum
Lateral septal nucleus, ventral part	LSv	Striatum
Septofimbrial nucleus	SF	Striatum
Septohippocampal nucleus	SH	Striatum
Anterior amygdalar area	AAA	Striatum
Bed nucleus of the accessory olfactory tract	BA	Striatum
Central amygdalar nucleus, capsular part	CEAc	Striatum
Central amygdalar nucleus, lateral part	CEAl	Striatum
Central amygdalar nucleus, medial part	CEAm	Striatum
Intercalated amygdalar nucleus	IA	Striatum
Medial amygdalar nucleus	MEA	Striatum
Globus pallidus, external segment	GPe	Pallidum
Globus pallidus, internal segment	GPi	Pallidum
Substantia innominata	SI	Pallidum
Magnocellular nucleus	MA	Pallidum
Medial septal nucleus	MS	Pallidum
Diagonal band nucleus	NDB	Pallidum
Triangular nucleus of septum	TRS	Pallidum
Bed nuclei of the stria terminalis	BST	Pallidum
Bed nucleus of the anterior commissure	BAC	Pallidum
Ventral anterior-lateral complex of the thalamus	VAL	Thalamus
Ventral medial nucleus of the thalamus	VM	Thalamus

Ventral posterolateral nucleus of the thalamus	VPL	Thalamus
Ventral posterolateral nucleus of the thalamus, parvicellular part	VPLpc	Thalamus
Ventral posteromedial nucleus of the thalamus	VPM	Thalamus
Ventral posteromedial nucleus of the thalamus, parvicellular part	VPMpc	Thalamus
Posterior triangular thalamic nucleus	PoT	Thalamus
Subparafascicular nucleus, magnocellular part	SPFm	Thalamus
Subparafascicular nucleus, parvicellular part	SPFp	Thalamus
Subparafascicular area	SPA	Thalamus
Peripeduncular nucleus	PP	Thalamus
Medial geniculate complex, dorsal part	MGd	Thalamus
Medial geniculate complex, ventral part	MGv	Thalamus
Medial geniculate complex, medial part	MGm	Thalamus
Dorsal part of the lateral geniculate complex, shell	LGd-sh	Thalamus
Dorsal part of the lateral geniculate complex, core	LGd-co	Thalamus
Dorsal part of the lateral geniculate complex, ipsilateral zone	LGd-ip	Thalamus
Lateral posterior nucleus of the thalamus	LP	Thalamus
Posterior complex of the thalamus	PO	Thalamus
Posterior limiting nucleus of the thalamus	POL	Thalamus
Suprageniculate nucleus	SGN	Thalamus
Ethmoid nucleus of the thalamus	Eth	Thalamus
Anteroventral nucleus of thalamus	AV	Thalamus
Anteromedial nucleus, dorsal part	AMd	Thalamus
Anteromedial nucleus, ventral part	AMv	Thalamus
Anterodorsal nucleus	AD	Thalamus
Interanteromedial nucleus of the thalamus	IAM	Thalamus
Interanterodorsal nucleus of the thalamus	IAD	Thalamus
Lateral dorsal nucleus of thalamus	LD	Thalamus
Intermediodorsal nucleus of the thalamus	IMD	Thalamus
Mediodorsal nucleus of thalamus	MD	Thalamus
Submedial nucleus of the thalamus	SMT	Thalamus
Perireunensis nucleus	PR	Thalamus
Paraventricular nucleus of the thalamus	PVT	Thalamus
Parataenial nucleus	PT	Thalamus
Nucleus of reuniens	RE	Thalamus
Xiphoid thalamic nucleus	Xi	Thalamus
Rhomboid nucleus	RH	Thalamus
Central medial nucleus of the thalamus	CM	Thalamus
Paracentral nucleus	PCN	Thalamus
Central lateral nucleus of the thalamus	CL	Thalamus
Parafascicular nucleus	PF	Thalamus
Posterior intralaminar thalamic nucleus	PIL	Thalamus
Reticular nucleus of the thalamus	RT	Thalamus
Intergeniculate leaflet of the lateral geniculate complex	IGL	Thalamus
Intermediate geniculate nucleus	IntG	Thalamus
Ventral part of the lateral geniculate complex	LGv	Thalamus
Subgeniculate nucleus	SubG	Thalamus
Medial habenula	MH	Thalamus
Lateral habenula	LH	Thalamus
Supraoptic nucleus	SO	Hypothalamus
Accessory supraoptic group	ASO	Hypothalamus
Paraventricular hypothalamic nucleus	PVH	Hypothalamus
Periventricular hypothalamic nucleus, anterior part	PVa	Hypothalamus
Periventricular hypothalamic nucleus, intermediate part	PVi	Hypothalamus
Arcuate hypothalamic nucleus	ARH	Hypothalamus

Anterodorsal preoptic nucleus	ADP	Hypothalamus
Anterior hypothalamic area	AHA	Hypothalamus
Anteroventral preoptic nucleus	AVP	Hypothalamus
Anteroventral periventricular nucleus	AVPV	Hypothalamus
Dorsomedial nucleus of the hypothalamus	DMH	Hypothalamus
Median preoptic nucleus	MEPO	Hypothalamus
Medial preoptic area	MPO	Hypothalamus
Vascular organ of the lamina terminalis	OV	Hypothalamus
Posterodorsal preoptic nucleus	PD	Hypothalamus
Parastrial nucleus	PS	Hypothalamus
Periventricular hypothalamic nucleus, posterior part	PVp	Hypothalamus
Periventricular hypothalamic nucleus, preoptic part	PVpo	Hypothalamus
Subparaventricular zone	SBPV	Hypothalamus
Suprachiasmatic nucleus	SCH	Hypothalamus
Subfornical organ	SFO	Hypothalamus
Ventromedial preoptic nucleus	VMPO	Hypothalamus
Ventrolateral preoptic nucleus	VLPO	Hypothalamus
Anterior hypothalamic nucleus	AHN	Hypothalamus
Lateral mammillary nucleus	LM	Hypothalamus
Medial mammillary nucleus, medial part	MMm	Hypothalamus
Medial mammillary nucleus, median part	Mmme	Hypothalamus
Medial mammillary nucleus, lateral part	MMl	Hypothalamus
Medial mammillary nucleus, posterior part	MMp	Hypothalamus
Medial mammillary nucleus, dorsall part	MMd	Hypothalamus
Supramammillary nucleus	SUM	Hypothalamus
Tuberomammillary nucleus, dorsal part	TMd	Hypothalamus
Tuberomammillary nucleus, ventral part	TMv	Hypothalamus
Medial preoptic nucleus	MPN	Hypothalamus
Dorsal premammillary nucleus	PMd	Hypothalamus
Ventral premammillary nucleus	PMv	Hypothalamus
Paraventricular hypothalamic nucleus, descending division	PVHd	Hypothalamus
Ventromedial hypothalamic nucleus	VMH	Hypothalamus
Posterior hypothalamic nucleus	PH	Hypothalamus
Lateral hypothalamic area	LHA	Hypothalamus
Lateral preoptic area	LPO	Hypothalamus
Preparasubthalamic nucleus	PST	Hypothalamus
Parasubthalamic nucleus	PSTN	Hypothalamus
Perifornical nucleus	PeF	Hypothalamus
Retrochiasmatic area	RCH	Hypothalamus
Subthalamic nucleus	STN	Hypothalamus
Tuberal nucleus	TU	Hypothalamus
Zona incerta	ZI	Hypothalamus
Fields of Forel	FF	Hypothalamus
Median eminence	ME	Hypothalamus
Superior colliculus, optic layer	SCop	Midbrain
Superior colliculus, superficial gray layer	SCsg	Midbrain
Superior colliculus, zonal layer	SCzo	Midbrain
Inferior colliculus, central nucleus	ICc	Midbrain
Inferior colliculus, dorsal nucleus	ICd	Midbrain
Inferior colliculus, external nucleus	ICe	Midbrain
Nucleus of the brachium of the inferior colliculus	NB	Midbrain
Nucleus sagulum	SAG	Midbrain
Parabigeminal nucleus	PBG	Midbrain
Midbrain trigeminal nucleus	MEV	Midbrain

Substantia nigra, reticular part	SNr	Midbrain
Ventral tegmental area	VTA	Midbrain
Midbrain reticular nucleus, retrorubral area	RR	Midbrain
Midbrain reticular nucleus	MRN	Midbrain
Superior colliculus, motor related, deep gray layer	SCdg	Midbrain
Superior colliculus, motor related, deep white layer	SCdw	Midbrain
Superior colliculus, motor related, intermediate white layer	SCiw	Midbrain
Superior colliculus, motor related, intermediate gray layer	SCig	Midbrain
Periaqueductal gray	PAG	Midbrain
Precommissural nucleus	PRC	Midbrain
Interstitial nucleus of Cajal	INC	Midbrain
Nucleus of Darkschewitsch	ND	Midbrain
Subcommissural organ	SCO	Midbrain
Anterior pretectal nucleus	APN	Midbrain
Medial pretectal area	MPT	Midbrain
Nucleus of the optic tract	NOT	Midbrain
Nucleus of the posterior commissure	NPC	Midbrain
Olivary pretectal nucleus	OP	Midbrain
Posterior pretectal nucleus	PPT	Midbrain
Retroparafascicular nucleus	RPF	Midbrain
Cuneiform nucleus	CUN	Midbrain
Red nucleus	RN	Midbrain
Oculomotor nucleus	III	Midbrain
Medial accesory oculomotor nucleus	MA3	Midbrain
Edinger-Westphal nucleus	EW	Midbrain
Trochlear nucleus	IV	Midbrain
Paratrochlear nucleus	Pa4	Midbrain
Ventral tegmental nucleus	VTN	Midbrain
Paranigral nucleus	PN	Midbrain
Anterior tegmental nucleus	AT	Midbrain
Lateral terminal nucleus of the accessory optic tract	LT	Midbrain
Dorsal terminal nucleus of the accessory optic tract	DT	Midbrain
Medial terminal nucleus of the accessory optic tract	MT	Midbrain
Substantia nigra, compact part	SNc	Midbrain
Posterior pretectal nucleus	PPN	Midbrain
Interfascicular nucleus raphe	IF	Midbrain
Interpeduncular nucleus, rostral	IPR	Midbrain
Interpeduncular nucleus, caudual	IPC	Midbrain
Interpeduncular nucleus, apical	IPA	Midbrain
Interpeduncular nucleus, lateral	IPL	Midbrain
Interpeduncular nucleus, intermediate	IPI	Midbrain
Interpeduncular nucleus, dorsomedial	IPDM	Midbrain
Interpeduncular nucleus, dorsolateral	IPDL	Midbrain
Interpeduncular nucleus, rostrolateral	IPRL	Midbrain
Rostral linear nucleus raphe	RL	Midbrain
Central linear nucleus raphe	CLI	Midbrain
Dorsal nucleus raphe	DR	Midbrain
Nucleus of the lateral lemniscus	NLL	Pons
Principal sensory nucleus of the trigeminal	PSV	Pons
Parabrachial nucleus	PB	Pons
Koelliker-Fuse subnucleus	KF	Pons
Superior olivary complex, periolivary region	POR	Pons
Superior olivary complex, medial part	SOCm	Pons
Superior olivary complex, lateral part	SOCl	Pons

Barrington's nucleus	B	Pons
Dorsal tegmental nucleus	DTN	Pons
Posterodorsal tegmental nucleus	PDTg	Pons
Pontine central gray	PCG	Pons
Pontine gray	PG	Pons
Pontine reticular nucleus, caudal part	PRNc	Pons
Supragenual nucleus	SG	Pons
Supratrigeminal nucleus	SUT	Pons
Tegmental reticular nucleus	TRN	Pons
Motor nucleus of trigeminal	V	Pons
Peritrigeminal zone	P5	Pons
Accessory trigeminal nucleus	Acs5	Pons
Parvicellular motor 5 nucleus	PC5	Pons
Intertrigeminal nucleus	I5	Pons
Superior central nucleus raphe	CS	Pons
Locus ceruleus	LC	Pons
Laterodorsal tegmental nucleus	LDT	Pons
Nucleus incertus	NI	Pons
Pontine reticular nucleus	PRNr	Pons
Nucleus raphe pontis	RPO	Pons
Subceruleus nucleus	SLC	Pons
Sublaterodorsal nucleus	SLD	Pons
Area postrema	AP	Medulla
Dorsal cochlear nucleus	DCO	Medulla
Ventral cochlear nucleus	VCO	Medulla
Cuneate nucleus	CU	Medulla
Gracile nucleus	GR	Medulla
External cuneate nucleus	ECU	Medulla
Nucleus of the trapezoid body	NTB	Medulla
Nucleus of the solitary tract	NTS	Medulla
Spinal nucleus of the trigeminal, caudal part	SPVC	Medulla
Spinal nucleus of the trigeminal, interpolar part	SPVI	Medulla
Spinal nucleus of the trigeminal, oral part	SPVO	Medulla
Paratrigeminal nucleus	Pa5	Medulla
Abducens nucleus	VI	Medulla
Facial motor nucleus	VII	Medulla
Accessory facial motor nucleus	ACVII	Medulla
Nucleus ambiguus, dorsal division	AMBd	Medulla
Nucleus ambiguus, ventral division	AMBv	Medulla
Dorsal motor nucleus of the vagus nerve	DMX	Medulla
Gigantocellular reticular nucleus	GRN	Medulla
Infracerebellar nucleus	ICB	Medulla
Inferior olivary complex	IO	Medulla
Intermediate reticular nucleus	IRN	Medulla
Inferior salivatory nucleus	ISN	Medulla
Linear nucleus of the medulla	LIN	Medulla
Lateral reticular nucleus, magnocellular part	LRNm	Medulla
Lateral reticular nucleus, parvicellular part	LRNp	Medulla
Magnocellular reticular nucleus	MARN	Medulla
Medullary reticular nucleus, dorsal part	MDRNd	Medulla
Medullary reticular nucleus, ventral part	MDRNv	Medulla
Parvicellular reticular nucleus	PARN	Medulla
Parasolitary nucleus	PAS	Medulla
Paragigantocellular reticular nucleus, dorsal part	PGRNd	Medulla

Paragigantocellular reticular nucleus, lateral part	PGRNl	Medulla
Nucleus of Roller	NR	Medulla
Nucleus prepositus	PRP	Medulla
Parapyramidal nucleus	PPY	Medulla
Lateral vestibular nucleus	LAV	Medulla
Medial vestibular nucleus	MV	Medulla
Spinal vestibular nucleus	SPIV	Medulla
Superior vestibular nucleus	SUV	Medulla
Nucleus x	x	Medulla
Hypoglossal nucleus	XII	Medulla
Nucleus y	y	Medulla
Nucleus raphe magnus	RM	Medulla
Nucleus raphe pallidus	RPA	Medulla
Nucleus raphe obscurus	RO	Medulla
Lingula (I)	LING	Cerebellum
Central lobule 2	CENT2	Cerebellum
Central lobule 3	CENT3	Cerebellum
Culmen 4,5	CUL4, 5	Cerebellum
Declive (VI)	DEC	Cerebellum
Folium-tuber vermis (VII)	FOTU	Cerebellum
Pyramus (VIII)	PYR	Cerebellum
Uvula (IX)	UVU	Cerebellum
Nodulus (X)	NOD	Cerebellum
Simple lobule	SIM	Cerebellum
Ansiform lobule 1	ANcr1	Cerebellum
Ansiform lobule 2	ANcr2	Cerebellum
Paramedian lobule	PRM	Cerebellum
Copula pyramidis	COPY	Cerebellum
Paraflocculus	PFL	Cerebellum
Flocculus	FL	Cerebellum
Fastigial nucleus	FN	Cerebellum
Interposed nucleus	IP	Cerebellum
Dentate nucleus	DN	Cerebellum
Vestibulocerebellar nucleus	VeCB	Cerebellum
vomeronasal nerve	von	Fiber tracts
olfactory nerve layer of main olfactory bulb	onl	Fiber tracts
lateral olfactory tract, body	lot	Fiber tracts
lateral olfactory tract, dorsal limb	lotd	Fiber tracts
anterior commissure, olfactory limb	aco	Fiber tracts
optic nerve	IIn	Fiber tracts
brachium of the superior colliculus	bsc	Fiber tracts
superior colliculus commissure	csc	Fiber tracts
optic chiasm	och	Fiber tracts
optic tract	opt	Fiber tracts
oculomotor nerve	IIIn	Fiber tracts
medial longitudinal fascicle	mlf	Fiber tracts
posterior commissure	pc	Fiber tracts
trochlear nerve	IVn	Fiber tracts
motor root of the trigeminal nerve	moV	Fiber tracts
sensory root of the trigeminal nerve	sV	Fiber tracts
spinal tract of the trigeminal nerve	sptV	Fiber tracts
facial nerve	VIIn	Fiber tracts
genu of the facial nerve	gVIIn	Fiber tracts
vestibulocochlear nerve	vVIIIn	Fiber tracts

trapezoid body	tb	Fiber tracts
dorsal acoustic stria	das	Fiber tracts
lateral lemniscus	ll	Fiber tracts
inferior colliculus commissure	cic	Fiber tracts
brachium of the inferior colliculus	bic	Fiber tracts
solitary tract	ts	Fiber tracts
cuneate fascicle	cuf	Fiber tracts
medial lemniscus	ml	Fiber tracts
cerebellar commissure	cbc	Fiber tracts
superior cerebelar peduncles	scp	Fiber tracts
superior cerebellar peduncle decussation	dscp	Fiber tracts
uncinate fascicle	uf	Fiber tracts
ventral spinocerebellar tract	sctv	Fiber tracts
middle cerebellar peduncle	mcp	Fiber tracts
inferior cerebellar peduncle	icp	Fiber tracts
dorsal spinocerebellar tract	sctd	Fiber tracts
arbor vitae	arb	Fiber tracts
supra-callosal cerebral white matter	scwm	Fiber tracts
corpus callosum, anterior forceps	fa	Fiber tracts
corpus callosum, external capsule	ec	Fiber tracts
corpus callosum, extreme capsule	ee	Fiber tracts
genu of corpus callosum	ccg	Fiber tracts
corpus callosum, posterior forceps	fp	Fiber tracts
corpus callosum, body	ccb	Fiber tracts
corpus callosum, splenium	ccs	Fiber tracts
corticospinal tract	cst	Fiber tracts
internal capsule	int	Fiber tracts
cerebal peduncle	cpd	Fiber tracts
pyramid	py	Fiber tracts
pyramidal decussation	pyd	Fiber tracts
external medullary lamina of the thalamus	em	Fiber tracts
optic radiation	or	Fiber tracts
auditory radiation	ar	Fiber tracts
nigrostriatal tract	nst	Fiber tracts
direct tectospinal pathway	tspd	Fiber tracts
doral tegmental decussation	dtd	Fiber tracts
crossed tectospinal pathway	tspc	Fiber tracts
rubrospinal tract	rust	Fiber tracts
ventral tegmental decussation	vtd	Fiber tracts
amygdalar capsule	amc	Fiber tracts
anterior commissure, temporal limb	act	Fiber tracts
cingulum bundle	cing	Fiber tracts
alveus	alv	Fiber tracts
dorsal fornix	df	Fiber tracts
fimbria	fi	Fiber tracts
medial corticohypothalmic tract	mct	Fiber tracts
columns of the fornix	fx	Fiber tracts
dorsal hippocampal commissure	dhc	Fiber tracts
ventral hippocampal commissure	vhc	Fiber tracts
angular path	ab	Fiber tracts
stria terminalis	st	Fiber tracts
commissural branch of stria terminalis	stc	Fiber tracts
medial forebrain bundle	mfb	Fiber tracts
supraoptic commissures	sup	Fiber tracts

supramammillary decussation	smd	Fiber tracts
principal mammillary tract	pm	Fiber tracts
mammilothalmic tract	mtt	Fiber tracts
mammillotegmental tract	mtg	Fiber tracts
mammillary peduncle	mp	Fiber tracts
stria medullaris	sm	Fiber tracts
fasciculus retroflexus	fr	Fiber tracts
habenular commissure	hbc	Fiber tracts
lateral ventricle	VL	Ventricles
subependymal zone	SEZ	Ventricles
choroid plexus	chpl	Ventricles
third ventricle	V3	Ventricles
cerebral aqueduct	AQ	Ventricles
fourth ventricle	V4	Ventricles
fourth ventricle, lateral recess	V4r	Ventricles
central canal, spinal cord/medulla	c	Ventricles

Table 2. Enriched gene expression patterns used to aid in delineating cortical areas

For each area listed, gene expression is indicated by qualitative accessment as low (x), moderate (xx), or strong (xxx) signal.

	Ctgf	Rbp4	Syt6	Grp	Crh	Glt25d2	Sim1	Cux2	Nr5a1	Rorb	Tlx3	Pvalb	Ntsr1	Chrna2	Scnn1a	Trib2	Gal
FRP	x	xx	x	xx			xx										
ORBm	x	xx	x	xx			x										
ORBvl	x	xx	x	xx	xxx												
ORBl	x	xx	x	xx		x		x	xx	x							
PL	x	xxx	x	xx			xxx										
ILA	x	xxx	x				xxx										
Ald	x	xx	x	xx							x						
Alv	x	xx	x	xx			xx										
Alp	x		x				xx										x
GU	x			x						x							x
VISC	x			x		xx				x							x
MOp	x	xx	xxx			xxx		x	xx	x	x	x					
MOs	x	xx	xxx	xxx		xxx			x		x	x					
ACAd	x	x		xx												x	
ACAv	x	x		xx												x	
RSPd	x	x	xxx									xx					
RSPv	x	x	xxx									xx					xx
RSPagl	x		xxx				x							xx			
SSp-bfd	x				xx			xxx	xxx	xxx	xx	xxx	xx		xxx	x	
SSp-ul	x		x			x		xxx	xxx	xxx	xxx	xxx	xx	xx	xxx	x	
SSp-ll	x		x			x		xxx	xxx	xxx	xxx	xxx	xx	xx	xxx	x	
SSp-tr	x		x			x		xxx	xxx	xxx	xxx	xxx	xx	xx	x	x	
SSp-m	x		x			xx		xxx	xxx	xxx	xxx	xxx	xx		xxx	x	
SSp-n	x							xxx	xxx	xxx	xxx	xxx	xx		xxx	x	
SSp-un	x							x	x	xxx	xxx	xx	xx	x	xxx	x	
SSs	x	x						xx	xx	xxx	xx	x	xx	x	cc	x	
AUDp	x	xx			xx			x	x	xxx	x	xxx	xxx	xxx	cc	x	x
AUDd	x							x	x	xx	x	x	xx	xx		x	x
AUDv	x	x						x	x	xx		x	xx	xxx		x	x
AUDpo	x							x	x	xx	x	x	xx	xx		x	x
TEa	x									x			x	xx			x

ECT	x													xx			
PERI	x			x										xx			
VISp	x	x			xx			xxx	xx	xxx	x	xxx	xxx		xx	xx	x
VISl	x				x			xx	x	xx	xxx	x	xx			x	x
VISli	x				x			x	x	xx	xxx	x	xx			x	x
VISpor	x	xx			x			x	x	xx	xxx	x	xx			x	x
VISpl	x	xx						x	x	xx	xxx	x	xx			x	
VISal	x					x		xx	x	xx	xxx	x	xx			x	
VISrl	x					xx		x	x	xx	xxx	x	xx			x	
VISpm	x	x	x			xx					xxx	x	xx	x		x	
VISam	x	x	x			xx					xxx	x	xx	x		x	
VISa	x					xx			xx							x	

Table 3. Connectivity data used for delineating cortical areas.

Target Area	Location of Injection Site (Image Series ID)
ORBm	PT (159331462, 159432479)
ORBvl	MD (267610466, 267928844), Ald (180709230), ORBvl (480994108)
ORBl	MD (168300739), MOs (166055636, 180916954), ORBl (112306316), SMT (268163228)
PL	BLA (113144533), MD (168301446, 267610466, 267928844), AM (146658170, 158840459), PH (175374275)
ILA	CLA (485846989), COAp (125802444, 182294687), PH (175374275), PT (305449231), PVT (183225830,278510903), RE (174957972)
Ald	Ald (112596790, 180709230, 313327028), CM (158841171), DMH (266174751), LA (117317884), MD (267607635), MOs (180916954,287995889), PH (175374275), VISC (180917660)
Alv	Alv (166153483), Ald (180709230), BLA (113144533), DMH (266174751), MD (168301446), MOs (180916954), PH (175374275)
Alp	BLA (113144533), DMH (266174751), LA (117317884), MD (267607635), MOs (180916954, 287995889), PH (175374275), VISC (180917660)
GU	GU (272737914, 299783689), PH (175374275), VIS C (180436360, 180917660), VM (267929554),VPMpc and VPLpc (162018169)
VISC	CM (158841171), PH (175374275), VIS C (180436360, 180917660), VPMpc and VPLpc (162018169)
MOp	LD (267608343, 305425490), MOs (166055636, 263242463), SSp (181819064, 249327301), SSs (113036264, 168163498), VAL (113884251), VM (267929554)
MOs	Ald (180709230), PO (146658879), SSp (249327301), SSs (113036264, 117298988, 120916102, 168163498), VM (267929554), VISrl (303616127)
ACAd	AM (146658170), AV (100142569), BLA (113144533), MD (168300739 , 267610466, 267928844)
ACAv	AM (146658170, 158840459), AV (175818392), BLA (113144533), MD (267610466, 267928844), RE (174957972)
RSPd	LD (267608343, 305425490)
RSPv	AV (100142569, 114427219, 175818392, 267609756)
RSPagl	AM (158840459, 167571459)
SSp-un	PO (146658879, 267999740)
SSs	PO (146658879, 267999740), SSs (120916102)
AUDp	AUDp (115958825, 120491896, 146858006), NB (113165340)
AUDd	AUDd (158314278)
AUDv	AUDp and AUDd (115958825), LP and MG (113846682, 182805258), MG (180520257, 178489574), NB (113165340), SSs (120916102)
AUDpo	AUDd (158314278)

TEa	LA (117317884, 120762196), LP (113846682, 182805258), NB (113165340, 182805258), PH (175374275), DMH (266174751)
ECT	COAp (182294687), DMH (266174751), LA (117317884, 120762196), LP (113846682, 182805258), PH (175374275)
PERI	COAp (182294687), LA (117317884), PERI (293702482)
VISa	SSs (120916102)

Table 4. Gene expression enriched in specific layers of isocortex

For each layer listed, gene expression is indicated for a particular Cre line by qualitative accessment as low (x), moderate (xx), or strong (xxx) signal.

Transgenic Line	Layer 1	Layer 2/3	Layer 4	Layer 5	Layer 6a	Layer 6b
Calb2-IRES-Cre		x		x		
Ctgf-2A-dgCre-neo						x
Chrna2-Cre-OE25				x		
Crh-IRES-Cre		xx		x		
Cux2-CreERT2	x	xx	xx			
Dlg3-Cre_KG118			x		xx	
Gal-Cre-K187		x	x		xx	
Glt25d2-Cre-NF107				xx		
Grp-Cre-KH288		xx		x		
Nr5a1-Cre			xxx			
Ntsr1-Cre			x		xxx	
Rorb-IRES2-Cre			xxx		x	x
Prkcd-GluCla-CFP-IRES-Cre			xx		x	
Pvalb-IRES-Cre		x	xx	xx	x	
Rbp4-Cre	x			xxx		
Scnn1a-Tag3-Cre			xxx		x	
Sim1-Cre_KJ18		xx				
Syt6-Cre-KI148-195994			x		xx	
Tac1-IRES2-Cre-D				x		
Tlx3-Cre			xx			
Trib2-2A-CreERT2-D	x		xx			

REFERENCES

Ding (2013) Comparative anatomy of the prosubiculum, subiculum, presubiculum, postsubiculum, and parasubiculum in human, monkey, and rodent. *Journal of Comparative Neurology*. 521:4145-4162.

Dong HW (2008) *Allen Reference Atlas: a digital color brain atlas of the C57BL/6J male mouse*. Hoboken, NJ: John Wiley & Sons.

Fonov V, Evans AC, Botteron K, Almli CR, McKinstry RC, Collins DL (2011) Brain Development Cooperative Group. Unbiased average age-appropriate atlases for pediatric studies. *Neuroimage* 54:313-327.

Garrett ME, Nauhaus I, Marshel JH, Callaway EM (2014) Topography and areal organization of mouse visual cortex. *Journal Neuroscience* 34:12587-12600.

Kuan L, Li Y, Lau C, Feng D, Bernard A, Sunkin SM, Zeng H, Dang C, Hawrylycz M, Ng L (2015) Neuroinformatics of the Allen Mouse Brain Connectivity Atlas. *Methods* 73:4-17.

Lein ES, Callaway EM, Albright TD, Gage FH (2005) Redefining the boundaries of the hippocampal CA2 subfield in the mouse using gene expression and 3-dimensional reconstruction. *Journal Comparative Neurology* 485:1-10.

Lein ES, Hawrylycz MJ, Ao N, Ayres M, Bensinger A, Bernard A, Boe AF, Boguski MS, Brockway KS, Byrnes EJ, Chen L, Chen L, Chen TM, Chin MC, Chong J, Crook BE, Czaplinska A, Dang CN, Datta S, Dee NR, Desaki AL, Desta T, Diep E, Dolbeare TA, Donelan MJ, Dong HW, Dougherty JG, Duncan BJ, Ebbert AJ, Eichele G, Estin LK, Faber C, Facer BA, Fields R, Fischer SR, Fliss TP, Frensley C, Gates SN, Glattfelder KJ, Halverson KR, Hart MR, Hohmann JG, Howell MP, Jeung DP, Johnson RA, Karr PT, Kawal R, Kidney JM, Knapik RH, Kuan CL, Lake JH, Laramee AR, Larsen KD, Lau C, Lemon TA, Liang AJ, Liu Y, Luong LT, Michaels J, Morgan JJ, Morgan RJ, Mortrud MT, Mosqueda NF, Ng LL, Ng R, Orta GJ, Overly CC, Pak TH, Parry SE, Pathak SD, Pearson OC, Puchalski RB, Riley ZL, Rockett HR, Rowland SA, Royall JJ, Ruiz MJ, Sarno NR, Schaffnit K, Shapovalova NV, Sivisay T, Slaughterbeck CR, Smith SC, Smith KA, Smith BI, Sodt AJ, Stewart NN, Stumpf KR, Sunkin SM, Sutram M, Tam A, Teemer CD, Thaller C, Thompson CL, Varnam LR, Visel A, Whitlock RM, Wohnoutka PE, Wolkey CK, Wong VY, Wood M, Yaylaoglu MB, Young RC, Youngstrom BL, Yuan XF, Zhang B, Zwingman TA, Jones AR (2007) Genome-wide atlas of gene expression in the adult mouse brain. *Nature* 445:168-176.

Marshel JH, Garrett ME, Nauhaus I, Callaway EM (2011) Functional specialization of seven mouse visual cortical areas. *Neuron* 72:1040–1054.

Martersteck EM, Hirokawa KE, Evarts M, Bernard A, Duan X, Li Y, Ng L, Oh SW, Ouellette B, Royall JJ, Stoecklin M, Wang Q, Zeng H, Sanes JR, Harris JA (2017) Diverse central projection patterns of retinal ganglion cells. *Cell Report*. 18:2058-2072.

Oh SW, Harris JA, Ng L, Winslow B, Cain N, Mihalas S, Wang Q, Lau C, Kuan L, Henry AM, Mortrud MT, Ouellette B, Nguyen TN, Sorensen SA, Slaughterbeck CR, Wakeman W, Li Y, Feng D, Ho A, Nicholas E, Hirokawa KE, Bohn P, Joines KM, Peng H, Hawrylycz MJ, Phillips JW, Hohmann JG, Wohnoutka P, Gerfen CR, Koch C, Bernard A, Dang C, Jones AR, Zeng H (2014) A mesoscale connectome of the mouse brain. *Nature* 508:207-214.

Paxinos G, Franklin KBJ (2001) *The Mouse Brain in Stereotaxic Coordinates*, Second edition. Elsevier Academic Press, San Diego, CA.

Quina LA, Harris J, Zeng H, Turner EE (2017) Specific connections of the interpeduncular subnuclei reveal distinct components of the habenulopeduncular pathway. *Journal of Comparative Neurology* 525:2632-2656.

Ragan T, Kim KH, Bahlmann, K, So PT (2004) Two-photon Tissue Cytometry. *Methods in Cell Biology* 75:23-39.

Ragan T, Sylvan JD, Kim KH, Huang H, Bahlmann K, Lee RT, So PT (2007) High-resolution whole organ imaging using two-photon tissue cytometry. *J Biomedical Optics* 12:014015.

Wang Q, Burkhalter A (2007) Area map of mouse visual cortex. *Journal Comparative Neurology* 502:339-357.

Wang Q, Gao E, Burkhalter A (2011) Gateways of ventral and dorsal streams in mouse visual cortex. *Journal Neuroscience* 31:1905-1918.

Wang Q, Sporns O, Burkhalter A (2012) Network analysis of corticocortical connections reveals ventral and dorsal processing streams in mouse visual cortex. *Journal Neuroscience*. 32:4386-4399.

Wang Q, Ng L, Harris JA, Feng D, Li Y, Royall JJ, Oh SW, Bernard A, Sunkin SM, Koch C, Zeng H (2017) Organization of the connections between claustrum and cortex in the mouse. *Journal of Comparative Neurol*ogy 525:1317-1346

Yushkevich PA, Piven J, Hazlett HC, Smith RG, Ho S, Gee JC, Gerig G (2006) User-guided 3D active contour segmentation of anatomical structures: Significantly improved efficiency and reliability. *Neuroimage* 31:1116-1128.